A Study of the Gas-Phase Reactivity of Neutral Alkoxy Radicals by Mass Spectrometry: α-Cleavages and Barton-Type Hydrogen Migrations

Georg Hornung, Christoph A. Schalley, Martin Dieterle, Detlef Schröder, and Helmut Schwarz*

Dedicated to Sir Derek H. R. Barton

Abstract: The reactivity of neutral alkoxy radicals in the absence of any interfering intermolecular interactions is investigated by means of the recently introduced method of neutral and ion decomposition difference (NIDD) spectra. These are obtained from quantitative analysis of the corresponding neutralization–reionization (NR) and charge reversal (CR) mass spectra. The following trends emerge: alkoxy radicals with short (C_1–C_3) or branched alkyl chains give rise to α-cleavage products, whereas longer-chained alkoxy radicals undergo 1,5-hydrogen migrations from carbon to oxygen, that is, Barton-type chemistry. This facile rearrangement has been studied in detail for *n*-pentoxy radicals by isotopic labeling experiments and computation at the Becke 3LYP/6-31G* level of theory. Further, the NIDD spectra of 3-methylpentoxy radicals permit for the first time the identification of the diastereoselectivity of the gas-phase hydrogen migrations. The results from the NIDD method are compared to those from earlier studies in the condensed phase. This new mass spectrometric approach is suggested as a tool for the examination of intramolecular reactions of free alkoxy radicals which can usefully complement theoretical studies.

Keywords
alkoxy radicals · Barton reaction · density functional calculations · mass spectrometry · radicals

Introduction

Ever since the discovery of specific 1,5-hydrogen migrations in alkoxy radicals, the so-called Barton reaction,[1] the reactivity[2] of alkoxy and related heteroatom-centered radicals has attracted special attention.[3] Alkoxy radicals play a crucial role in the oxidation of alkanes, for example in combustion and atmospheric processes.[4] However, experimental studies of the reactivity of alkoxy radicals in solution are quite demanding in terms of analytical techniques and manpower.[5] Here, we describe a simple mass spectrometric approach for the investigation of some aspects of the intramolecular reactivity of gaseous alkoxy radicals.

Over the last two decades, mass spectrometry has developed from a mere analytical method to a sophisticated means for the gas-phase investigation of both unimolecular and collision-induced ion fragmentations, and of bimolecular ion–molecule reactions.[6] Since the mass analysis relies on the interaction of the charge with magnetic and electrostatic sectors, the method has long been limited to the examination of ionic species. However, in the late 1960s Lavertu et al. and Devienne[7] demonstrated that collisions of fast-moving ions with appropriate target gases can lead to the formation of transient neutral molecules. The pioneering work of McLafferty and coworkers developed neutralization–reionization (NR) mass spectrometry[8] into a general technique for structural characterization of unconventional neutral species generated from appropriate ionic precursors by vertical electron transfer.[9] Most often, this method has been used to address the existence and structural characterization of neutral species, and until now only a few studies[8a, h, 10] have dealt with the *reactivity* of the neutral species, most of them using the advantages of variable-time NR experiments.[10b] It is indeed often difficult to recognize which fragmentations in a NR experiment occur in the neutral species itself, since the projectile and recovery ions also undergo fragmentations. Recently, we developed a fairly simple approach to separate these phenomena by subtracting normalized charge reversal (CR)[11] spectra from NR spectra.[12] This method relies on the difference in fragmentation intensities of charged and neutral species, and thus has been denoted neutral and ion decomposition difference (NIDD) mass spectrometry.[13]

Here, we examine the gas-phase reactivity of alkoxy radicals by means of the NIDD method. As solution chemistry of alkoxy radicals has been studied in great detail by a variety of experimental[1–4] and theoretical[14] techniques, the present results will also serve to evaluate the performance of the NIDD method. The timescale of NR experiments (ca. 10^{-6} s) is quite

[*] Prof. Dr. H. Schwarz, Dr. D. Schröder, Dr. C. A. Schalley, Dipl.-Chem. G. Hornung, Dipl.-Chem. M. Dieterle
Institut für Organische Chemie der Technischen Universität Berlin
Strasse des 17. Juni 135, D-10623 Berlin (Germany)
Fax: Int. code +(30)314-21102
e-mail: schw0531@www.chem.tu-berlin.de

0947-6539/97/0311-1866 $ 17.50+.50/0

suitable for studying typical alkoxy radical fragmentations, such as α-cleavage of C–H or C–C bonds.[15] In addition, for alkoxy radicals with sufficiently long side chains, the regio- and diastereoselectivity of 1,5-hydrogen migrations (the Barton reaction)[1, 4] can be probed in the highly diluted gas phase by the NIDD method for substrates bearing a specific isotopic label.

Experimental Section

The experiments were performed with a modified VG ZAB/HF/AMD four-sector mass spectrometer of BEBE configuration (B stands for magnetic and E for electric sectors), which has been described in detail previously.[16] Briefly, for the generation of the alkoxide ions, mixtures of the corresponding alcohols and N_2O were ionized in a chemical ionization source (repeller voltage ≈0 V) with a beam of electrons of 50–100 eV kinetic energy. For $^-NR^-$ experiments,[17] which require rather large ion abundances, the alkoxide ions were made by negative-ion chemical ionization (NICI) of the corresponding trimethyl silyl ethers in a NF_3 plasma.[18] This method increases the alkoxide ion intensities significantly, because defluorosilylation occurs with high selectivity and the undesired formation of enolate ions by dehydrogenation of the alkoxides within the source is thus largely reduced.[11, 18]

The ions of interest were accelerated to 8 keV translational energy and mass-selected by means of B(1)/E(1) at mass resolutions of $m/\Delta m = 2000–5000$. Unimolecular decompositions of metastable alkoxide ions (MI) occurring in the field-free section preceding E(1) were recorded with this sector. For collisional activation (CA) experiments,[19] the ions were made to collide with helium in the field-free region preceding B(2) at 80% transmission (T) of the incident beam, which corresponds approximately to single-collision conditions.[20] The fragmentations were monitored with B(2).

In neutralization–reionization ($^-NR^+$) experiments, the alkoxide ions were neutralized by high-energy collisions with molecular oxygen (80% T) in the first of two differentially pumped collision cells located in the field-free region between E(1) and B(2). Unreacted ions were deflected away from the beam of neutral species by applying a voltage of 1 kV on a deflector electrode located between the two collision chambers. Subsequent reionization to cations occurred in a second cell by collisions with oxygen (80% T). The resulting mass spectra were recorded by scanning B(2). Due to the reduced total ion currents in $^-NR^-$ experiments, these were performed in the field-free region between B(1) and E(1). To this end, the ions were mass-selected with B(1), neutralized with O_2 (80% T), and reionized with benzene (70% T) in the field-free region preceding E(1), while this sector was scanned. Charge-reversal mass spectra[11] of alkoxide ions to cations ($^-CR^+$) were obtained by colliding the ion beam with oxygen (80% T) in the field-free region preceding B(2). It should be noted that under these conditions two-electron oxidations occur in a single step, although some of the ions undergo multiple collisions. Therefore, a small contribution of NR processes is inherent in the CR mass spectra. In order to study any possible perturbation of the NIDD spectra by multiple collisions (see below), the pressure of the target gas in the $^-CR^+$ experiments was systematically varied between 90–60% T. For the alkoxide ions under study, no distinct sensitivity towards collision gas pressure was observed, with one exception: the intensity of the $CO^{\bullet+}$ signal in the $^-CR^+$ mass spectra of the alkoxide ions increases with rising collision gas pressure. A detailed explanation for this behavior is discussed below. Charge-reversal/collisional activation ($^-CR^+$/CA) mass spectra of alkoxide ions were obtained by colliding the charge-reversed ion beam with helium (80% T) in the field-free region following B(2) and scanning the electric sector E(2).

All mass spectra were accumulated and processed online with the AMD-Intectra data system; usually, 20 to 100 scans were averaged to improve the signal-to-noise ratio. The $^-NIDD^+$ spectra were obtained by subtracting the normalized peak heights of the ions in the raw data files of the CR^+ spectra from those of the corresponding $^-NR^+$ spectra according to Equation (1).

$$I_i(\mathrm{NIDD}) = [I_i(\mathrm{NR})/\textstyle\sum_i I_i(\mathrm{NR})] - [I_i(\mathrm{CR})/\sum_i I_i(\mathrm{CR})] \quad (1)$$

The error bars of the resulting difference spectra are of course larger than those of the individual CR and NR spectra. To evaluate the reproducibility of the results, each NIDD spectrum reported below was independently checked at least once.

The unlabeled alcohols and their trimethylsilyl derivatives, which served as precursors for the generation of the corresponding alkoxide ions **1**–**8**, were either commercially available or synthesized, purified by distillation or preparative gas chromatography, and identified by ^1H NMR as well as mass spectrometry. The deuterated alcohols were made by reduction of the corresponding carbonyl compounds with either $LiAlH_4$ or $LiAlD_4$ (Aldrich Chemicals, >98% D). For example, CD_3CH_2OH was prepared by reduction of CD_3COOD with $LiAlH_4$ in diethyl ether, then the ether was removed from the reaction mixture under vacuum, the residue was treated with a small excess of saturated Na_2SO_4 solution (−78 → 0 °C), and the product was isolated by distillation and subsequently further purified. Similarly, [4,4,4-D_3]1-butanol was prepared by a) treatment of acetic acid with lithium diisopropyl amide (LDA) in tetrahydrofuran to yield the dianion, b) alkylation of the dianion with CD_3CH_2Br, followed by aqueous workup and the isolation of [4,4,4-D_3]butyric acid, and c) reduction of the labeled acid with $LiAlH_4$, work-up with saturated NH_4Cl solution, and isolation of the desired alcohol. In an analogous manner, **8b**–**8d** were prepared. For example, **8b** was synthesized by a) treatment of propionic acid with LDA in tetrahydrofuran to yield the corresponding dianion, b) alkylation of the dianion with CH_3CD_2Br followed by isolation of [3,3-D_2]2-methylbutyric

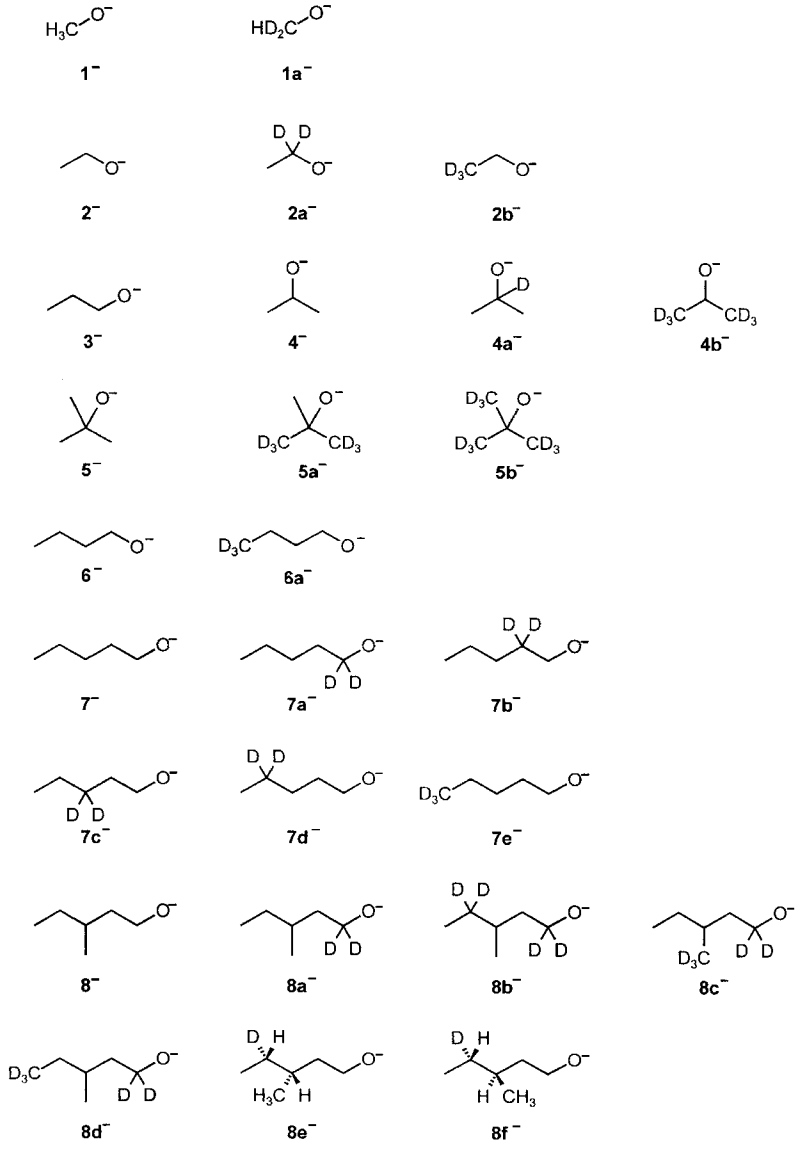

acid, c) reduction of this acid with $LiAlH_4$ and conversion of the alcohol obtained to the bromide by treatment with HBr, d) generation of the corresponding Grignard reagent, which was converted to [4,4-D_2]3-methylpentanoic acid by reaction with CO_2, and finally, e) reduction of the acid with $LiAlD_4$ followed by conventional aqueous work-up and distillation.

The diastereoselectively labeled [4-D_1]3-methylpentan-1-ols **8e** and **8f** were prepared as racemic pairs starting from commercially available *cis*- and *trans*-butene (Linde AG, 98% purity), respectively (Scheme 1), via a) epoxidation

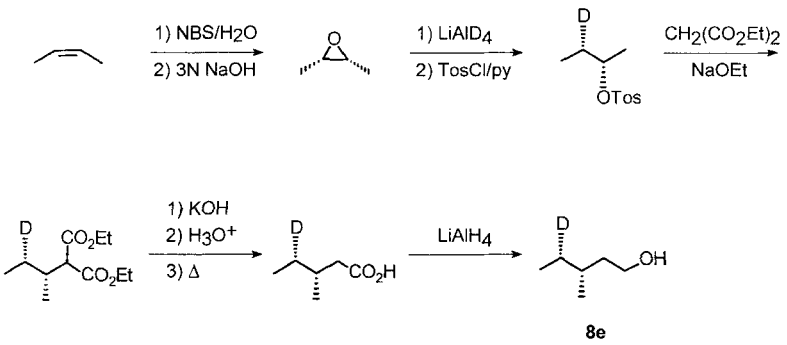

Scheme 1. Preparation of diastereoselectively labeled [4-D_1]3-methylpentan-1-ol.

with NBS under basic conditions, b) reduction of the epoxides with $LiAlD_4$, c) tosylation of the corresponding [3-D_1]2-butanols, d) subsequent nucleophilic displacement by diethyl malonate, e) saponification of the resulting diesters with aqueous KOH, f) thermal decarboxylation of the diacids, and g) reduction of the carboxylic acids with $LiAlH_4$.

Computational details: The calculations were carried out with the hybrid DFT/HF Becke 3LYP method, as implemented in Gaussian 94,[21] using the standard 6-31G* basis set for all atoms.[22] Geometry optimizations were performed with gradient procedures, and vibrational frequencies were calculated in order to determine the nature of stationary points. The unscaled[12,3] frequencies were also used to derive zero-point vibrational energy (ZPVE) corrections. All energies are given as heats of formation instead of relative energies. As an anchor point, the experimental value for protonated 2-methyltetrahydrofuran ($\Delta H_f = 110.0$ kcal mol^{-1}) has been chosen.[24] Selected geometrical data for calculated species are indicated in Schemes 5 and 6. A complete set of Cartesian coordinates for each of the species is given in ref. [12d] and is available upon request.

In general, the Becke 3LYP approach is expected to provide an accuracy of ca. ± 5 kcal mol^{-1} for relative energies;[25] nevertheless, the level of theory applied here does not reproduce well the electron affinity (EA) of the pentoxy radical as derived from literature data. The calculated value of 0.96 eV is only about half of the EA(*n*-$C_5H_{11}O^{\cdot}$) of ca. 2 eV as extrapolated from the literature data[24] for methoxy (1.59 eV), ethoxy (1.72 eV), *n*-propoxy (1.79 eV), and *n*-butoxy (1.90 eV) radicals. This failure is certainly due to the basis set used, which is not appropriate for a quantitative prediction of electron affinities, and diffuse basis functions have to be added for this purpose.[26] However, this is no serious drawback in the present context, because the crucial processes that determine structure and reactivity and which form the focus of the present study take place on the neutral and cationic surfaces. As will be shown by comparison of the theoretical results with known experimental data for several key species (see below), the level of theory and the corresponding basis set chosen are appropriate for a qualitative, if not semiquantitative description of these systems. Therefore, the problem of an accurate computational evaluation of electron affinities was not further pursued here.

Results and Discussion

This paper uses a new mass-spectrometric approach to study the reactivity of neutral organic radicals. This approach, the NIDD technique, was introduced in ref. [13], to which the interested reader is referred for an in-depth methodological description. Some key aspects of the $^-$NIDD$^+$ variant used in this study of importance for the understanding of the present results are discussed in the next section.

The $^-$NIDD$^+$ method: The method relies on the comparison of mass spectral data from neutralization–reionization ($^-$NR$^+$; Figure 1a) and charge reversal ($^-$CR$^+$; Figure 1b). In a $^-$CR$^+$ experiment, a mass-selected, fast-moving anion (usually with a kinetic energy in the keV range) is made to collide with a target gas, and the following analyzer is adjusted to transmit positive ions so that charge-reversed species are detected. The vast majority of $^-$CR$^+$ events involve vertical, two-electron transfer processes to yield the corresponding cations.

In a $^-$NR$^+$ experiment (Figure 1a), the mass-selected anion is subjected to two sequential collision events, in both of which a one-electron transfer process occurs. In the first collision, the

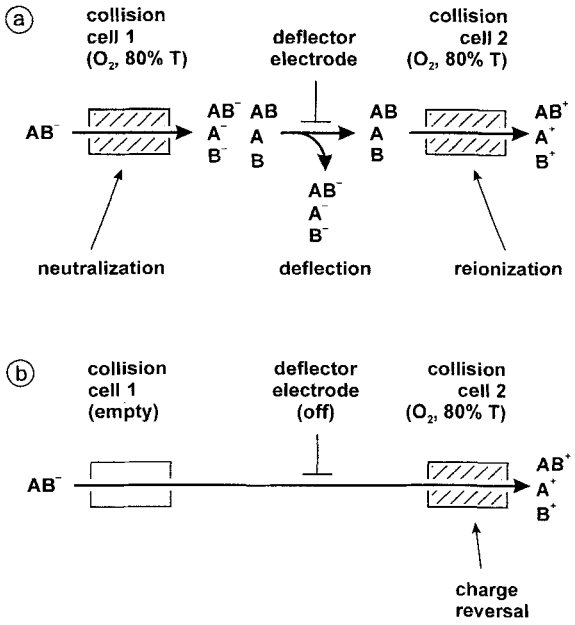

Figure 1. Schematic representation of a) $^-$NR$^+$ and b) $^-$CR$^+$ experiments.

anion yields the corresponding neutral species and the remaining ions are deflected away by a high voltage of ca. 1 kV. The neutral can travel freely for a distance of some cm, which corresponds to a lifetime of the order of several microseconds. A second collision leads to reionization of the fast-moving neutral beam to give cations which are then detected by conventional mass spectrometric techniques. The key feature of the NIDD approach is that in a $^-$NR$^+$ experiment, unimolecular reactions and fragmentations of the neutral(s) may take place in the μs time interval preceding reionization, while these do not occur in the $^-$CR$^+$ event. Hence, the product ions may differ, yielding information on the processes taking place in the neutrals. In other words, CR spectra are dominated by fragmentations of ionic species, while NR spectra also contain contributions from the fragmentations of the neutral intermediates. The contributions of the neutral and the ionic species can be identified by

0947-6539/97/0311-1868 $ 17.50+.50/0 Chem. Eur. J. 1997, 3, No. 11

subtracting the normalized CR spectrum from the normalized NR spectrum. This yields a NIDD mass spectrum, in which the positive intensities correspond to the fragmentation of neutrals, while ionic fragmentations appear as negative peaks.

From these considerations, some conditions can be derived for the application of this approach.

a) Only those ions can be studied which give rise to structurally indicative CR spectra. While this may be a drawback for the investigation of cationic precursors, the $^-CR^+$ procedure is expected to be applicable to almost any anionic species.[13]
b) The neutral under study has to be formed as a major component of the particle beam in the neutralization event. This can be checked by recording $^-NR^-$ mass spectra, in which intense recovery signals should be present.
c) The internal energies and lifetimes of the neutrals formed should fit the time window of the experiment. Thus, unstable neutrals which decompose immediately after neutralization or neutrals which are stable in the μs timeframe will not give meaningful NIDD spectra.
d) The systems under study should not be very sensitive to the pressure of target gases in the collision cells. This is of particular importance, because the CR procedure requires only one collision, while two collisions are needed for a NR experiment. A strong sensitivity of the spectra to the collision conditions may give rise to artifacts in the NIDD spectra.
e) The reactivity of the reionized species should not be too sensitive to changes in internal energy, because this would be reflected in additional differences between the NR and CR mass spectra.[12a] Such changes in internal energy may occur because of the vertical nature of the electron-transfer processes.
f) Finally, the nature of NIDD mass spectrometry as a difference method requires high reproducibility of CR and NR spectra.

The application of $^-NIDD^+$ to alkoxide ions: Exploratory experiments demonstrated that the requirements defined above hold true for this class of compounds. In particular, the $^-CR^+$ and $^-NR^+$ spectra of alkoxide ions are well reproducible and show a distinct dependence on the structure of the precursors.[27] Further, $^-NR^-$ mass spectra (see below) of alkoxide ions confirm that the neutral alkoxy radicals are formed as major components such that fragmentation of the anions hardly interferes. Finally, except for the $CO^{\bullet+}$ signal (see below), the $^-CR^+$ mass spectra are barely sensitive towards collision gas pressures. Hence, all prerequisites are fulfilled for the alkoxides, so $^-CR^+$ and $^-NR^+$ experiments can be performed and the normalized spectra subtracted from each other to afford the corresponding $^-NIDD^+$ spectra. Two major advantages of the NIDD approach should be mentioned. a) The measurements do not demand special instrumentation as needed for variable-time NR experiments.[10b] b) NR and CR experiments can be carried out directly one after the other while ion source and focus conditions can be kept constant, thereby eliminating several possible error sources.

The gas-phase chemistry of neutral alkoxy radicals: α-C–H and α-C–C bond cleavage: As we are proposing an entirely new approach to investigate the reactivity of alkoxy radicals in the gas phase, let us dwell upon the parent system, the methoxy radical, in more detail. In 1979, Bursey et al.[27] reported the $^-CR^+$ spectra of several alkoxide ions. From a comparison with the CA mass spectra of independently generated cationic isomers they concluded that alkoxy cations with an electron-deficient oxygen atom are produced upon charge inversion. Five years later, Burgers and Holmes[28] showed that singlet methoxy cations, $^1CH_3O^+$, rearrange without a barrier to the hydroxymethyl cations, $^1CH_2OH^+$, while the much less stable triplet electromer $^3CH_3O^+$ rests in a shallow minimum on the $^3[C,H_3,O]^+$ potential energy surface.[29] Collisional activation of mass-selected survivor ions in a $^-CR^+$/CA experiment unravels the methoxy connectivity: fragments at $m/z = 15$ and 16 indicate the presence of a methyl group and an oxygen atom, whereas a signal at $m/z = 17$ is negligible. The CH_2OH^+ isomer instead gives rise to signals at $m/z = 14$ and 17, while almost no peak is detected at $m/z = 15$.

The $^-NR^+$ (Figure 2a) and $^-CR^+$ (Figure 2b) mass spectra of the methoxide ion $\mathbf{1}^-$ reveal very similar intensity distributions. Notable differences are only observed for the losses of

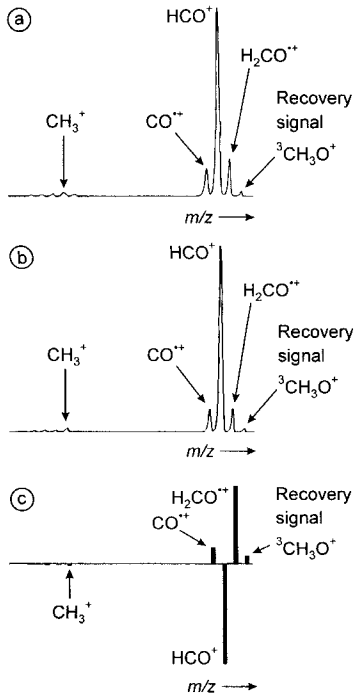

Figure 2. a) $^-NR^+$ mass spectrum (O_2, 80% T; O_2, 80% T), b) $^-CR^+$ mass spectrum (O_2, 80% T), and c) $^-NIDD^+$ spectrum of methoxide ions $\mathbf{1}^-$.

atomic and molecular hydrogen (m/z 30 and 29, respectively; Table 1). Considering the electron affinity of 1.59 eV for the methoxy radical,[24] electron loss should be a relatively facile process in the collisions of fast $\mathbf{1}^-$ with a target gas such that methoxy radicals will be produced as the major component of the neutral beam. This conjecture is supported by the $^-NR^-$ spectrum of $\mathbf{1}^-$, in which the survivor signal for reionized CH_3O^- represents the base peak. Furthermore, the $^-CR^+$ mass spectrum hardly depends on collision gas pressure.

Subtraction of the normalized $^-CR^+$ intensities (Table 1, entry 2) from the $^-NR^+$ peak heights (entry 1) leads to the

  0947-6539/97/0311-1869 $ 17.50+.50/0

Table 1. Mass differences (in amu) observed in the $^{-}NR^{+}$ and $^{-}CR^{+}$ mass spectra (entries 1 and 2) of methoxide ions ($\mathbf{1}^{-}$) and $^{-}NIDD^{+}$ mass spectrum (entry 3). The intensities of the $^{-}NR^{+}$ and $^{-}CR^{+}$ mass spectra are normalized to the sum of all fragmentations equal to unity including the recovery signal.

Entry		*m/z*									Σ
		31	30	29	28	16	15	14	13	12	
1	$^{-}NR^{+}$	0.020	0.142	0.688	0.105	0.007	0.015	0.010	0.007	0.006	1
2	$^{-}CR^{+}$	0.015	0.095	0.754	0.096	0.004	0.016	0.008	0.007	0.005	1
3	$^{-}NIDD^{+}$	0.005	0.047	−0.066	0.009	0.003	−0.001	0.002	0.000	0.001	0

$^{-}NIDD^{+}$ spectrum listed in entry 3 of Table 1 and in Figure 2c. The most important feature is that the signal for $CH_2O^{\bullet+}$ is positive, indicating that the loss of a hydrogen atom occurs from neutral $CH_3O^{\bullet}$. From the $^{-}NIDD^{+}$ spectrum of isotopomer $\mathbf{1a}^{-}$ a primary kinetic isotope effect of $k_H:k_D = 2.1$ for the loss of atomic hydrogen can be derived. In contrast, the elimination of molecular hydrogen to give rise to HCO^{+} appears with negative intensity; this is in line with the known fact that dehydrogenation proceeds after reionization to the methoxy cation.[28] Also, the $^{-}CR^{+}$ mass spectrum exhibits a signal (though weaker) for the loss of atomic hydrogen. This finding can be traced back to two processes: a) A small quantity of neutral species is generated in the charge reversal procedure (see Experimental Section), and their fragmentations obviously contribute to the observed spectrum. b) In addition, part of the $CH_2O^{\bullet+}$ signal observed in the CR spectrum is due to collision-induced fragmentations of the reionized methoxy cations. This is in agreement with the observation of a small $CH_2O^{\bullet+}$ signal ($\approx 10\%$ relative to the base peak) in the $^{-}CR^{+}$/CA mass spectrum, in which the recovered methoxy cation is mass-selected and collisionally activated. Nevertheless, the positive signal observed for $CH_2O^{\bullet+}$ in the $^{-}NIDD^{+}$ spectrum gives evidence that the major contribution is due to neutral $CH_3O^{\bullet}$. Instead, the major process in the $^{-}CR^{+}$/CA mass spectrum corresponds to loss of H_2. This indicates that the formation of HCO^{+} occurs from reionized CH_3O^{-} fully in line with the negative $^{-}NIDD^{+}$ signal for this ion.

In conclusion, the result of the $^{-}NIDD^{+}$ experiment can be summarized in a simple picture (Scheme 2, $R^1 = R^2 = R^3 = H$): on neutralization of the anion, the methoxy radical undergoes loss of atomic hydrogen by α-C–H bond cleavage, yielding formaldehyde as the favorable neutral product. In contrast, the negative signal for *m/z* 29 (HCO^{+}) in Figure 2c implies that 1,1-elimination of molecular hydrogen from the radical is not significant, and rather prevails for the cationic species.

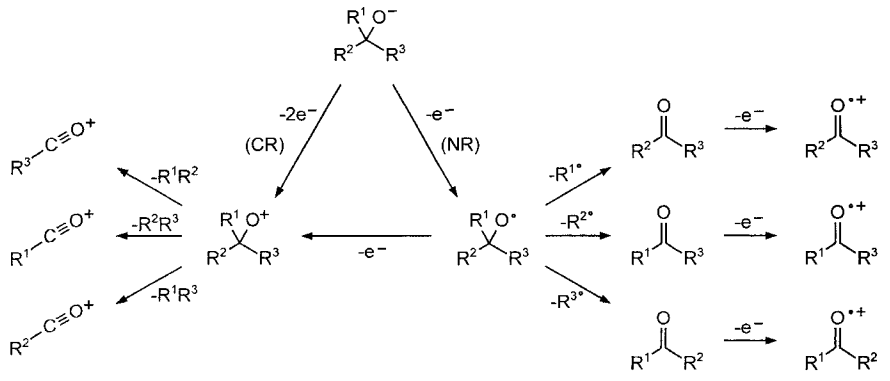

Scheme 2. Interpretation of the $^{-}NIDD^{+}$ spectrum in Figure 2c.

Let us now briefly return to the origin of the $CO^{\bullet+}$ signal, which shows up in the $^{-}NIDD^{+}$ spectrum as a positive peak. In the $^{-}CR^{+}$ experiment, this signal increases with rising collision gas pressure. An earlier NR study of acetaldehyde radical cations[30] reported that the $CO^{\bullet+}$ signal is due to loss of CH_4 at the neutral stage. In addition, a strong pressure dependence of this particular signal is observed when the neutral is collisionally activated in an NCR (neutralization–collisional activation of the neutral–reionization) experiment, in perfect agreement with our observations. Thus, in the case of alkoxy radicals, the $CO^{\bullet+}$ signal can be rationalized by consecutive fragmentation consisting of α-cleavage leading to formation of a neutral carbonyl moiety, which further decomposes to give rise to CO, subsequently detected as its radical cation after reionization.

The observed reactivity of the neutral fully agrees with thermochemical considerations (Table 2). Methoxy radicals can, in principle, decompose by two different bond cleavage reactions

Table 2. Heats of reaction (ΔH_r) for several fragmentation reactions of alkoxy radicals. Energies are given in kcal mol^{-1} [a].

Reaction		ΔH_r
$CH_3O^{\bullet}$	→ $CH_2O + H^{\bullet}$	22.4
$CH_3O^{\bullet}$	→ $CH_3^{+} + O$	90.7
$CH_3O^{\bullet}$	→ $HCO^{\bullet} + H_2$	7.0 [b]
$CH_3O^{\bullet}$	→ $CH^{\bullet} + H_2O$	80.9 [b]
$CH_3O^{\bullet}$	→ $CH_2 + OH^{\bullet}$	98.6 [b]
$CH_3CH_2O^{\bullet}$	→ $CH_2O + CH_3^{+}$	13.0
$CH_3CH_2O^{\bullet}$	→ $CH_3CHO + H^{\bullet}$	16.7
$CH_3CH_2CH_2O^{\bullet}$	→ $CH_2O + CH_3CH_2^{+}$	11.9
$CH_3CH_2CH_2O^{\bullet}$	→ $CH_3CH_2CHO + H^{\bullet}$	17.2
$(CH_3)_2CHO^{\bullet}$	→ $CH_3CHO + CH_3^{+}$	7.7
$(CH_3)_2CHO^{\bullet}$	→ $(CH_3)_2CO + H^{\bullet}$	12.7
$(CH_3)_3CO^{\bullet}$	→ $(CH_3)_2CO + CH_3^{+}$	5.7

[a] Calculated on the basis of literature data.[24] [b] These reactions do not correspond to simple bond cleavages, and the presence of a barrier has to be taken into account (see text).

Rupture of one of the C–H bonds to afford $CH_2O + H^{\bullet}$ is endothermic (22.4 kcal mol^{-1}). In comparison, cleavage of the C–O bond is much more energetically demanding (90.7 kcal mol^{-1}); consequently, this process does not contribute to the observed radical reactions. The formation of an $HCO^{\bullet}$ radical concomitant with H_2 is located energetically below the $H^{\bullet}$ loss (7.0 versus 22.4 kcal mol^{-1}). However, in the neutral species the calculated barrier for the H_2 elimination reaction exceeds that for hydrogen-atom loss by more than 20 kcal mol^{-1}.[31] Finally, the formation

0947-6539/97/0311-1870 $ 17.50+.50/0 *Chem. Eur. J.* **1997**, *3*, No. 11

of $CH^{\bullet} + H_2O$ (80.9 kcal mol^{-1}) and of $CH_2 + OH^{\bullet}$ (98.6 kcal mol^{-1}) can also be ruled out for energetic reasons. In conclusion, the loss of hydrogen atoms from methoxy radicals is the process of lowest energy demand, which is in good agreement with the experimental findings and literature data.[3, 15]

In order to probe whether the reactivity pattern depicted in Scheme 2 can be generalized, a series of alkoxide ions (**1**–**8**) was investigated by means of the $^{-}$NIDD^{+} approach. Neutral ethoxy radicals **2**$^{\bullet}$ ($R^1 = R^2 = H$; $R^3 = CH_3$) give rise to methyl loss competing with hydrogen-atom expulsion. The loss of $CH_3^{\bullet}$ is somewhat less endothermic (13.0 kcal mol^{-1}, Table 2) than the expulsion of a hydrogen atom (16.7 kcal mol^{-1}). This thermochemistry is in line with the experimental observation (Figure 3a) that more $CH_3^{\bullet}$ than H$^{\bullet}$ is expelled from **2**$^{\bullet}$. In contrast, ethoxy cations yield predominantly HCO^+ concomitant with methane formation by 1,1-elimination. In addition, a less intense 1,1-elimination of H_2 is found supporting the reactivity pattern as displayed in Scheme 2. These conjectures are further supported by the $^{-}$NIDD^{+} spectra of the isotopomers **2a**$^{\bullet}$ and **2b**$^{\bullet}$ (Figures 3b,c). Their $^{-}$NIDD^{+} spectra reveal that neutral **2a**$^{\bullet}$ exhibits losses of D$^{\bullet}$ and $CH_3^{\bullet}$, whereas **2b**$^{\bullet}$ expels H$^{\bullet}$ and $CD_3^{\bullet}$. In addition, DCO^+ and HCO^+, respectively, represent the products of the 1,1-eliminations of CH_3D and CD_3H from these isotopomers at the ionic stage.[32]

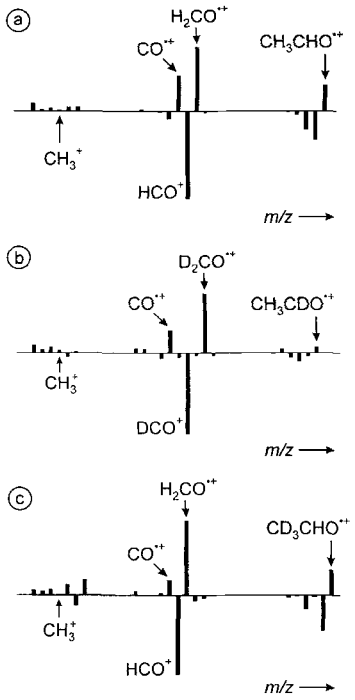

Figure 3. a) $^{-}$NIDD^{+} spectrum of ethoxide ions **2**$^{-}$. b) $^{-}$NIDD^{+} spectrum of [1-D$_2$]ethoxide ions **2a**$^{-}$, and c) $^{-}$NIDD^{+} spectrum of [2-D$_3$]ethoxide ions **2b**$^{-}$.

Analogous reactivity was observed for the radicals **3**$^{\bullet}$, **4**$^{\bullet}$, and **5**$^{\bullet}$ generated from the corresponding alkoxide ions. For example, neutral *n*-propoxy radicals **3**$^{\bullet}$ ($R^1 = R^2 = H$; $R^3 = CH_2CH_3$) give rise to ethyl loss in conjunction with a small amount of hydrogen-atom expulsion. The loss of $C_2H_5^{\bullet}$ is 5.3 kcal mol^{-1} (Table 2) less endothermic than the expulsion of a hydrogen atom, fully in line with the experimentally observed intensities in the $^{-}$NIDD^{+} mass spectrum (Figure 4a). In contrast, for *n*-propoxy cations a strong HCO^+ signal corresponding to the loss of C_2H_6 by a 1,1-elimination reaction is observed. In addition, a less intense 1,1-elimination of H_2 is also found. The $^{-}$NIDD^{+} mass spectrum of *i*-propoxide **4**$^{-}$ (Figure 4b) reveals that the formation of acetone and acetaldehyde by elimination of H$^{\bullet}$ and $CH_3^{\bullet}$, respectively, proceeds during the neutral stage prior to reionization. As the difference of the reaction enthalpies for H$^{\bullet}$ ($\Delta H_r = 16.7$ kcal mol^{-1}; Table 3) and $CH_3^{\bullet}$ losses ($\Delta H_r = 7.7$ kcal mol^{-1}) is larger than in the ethoxy system, the hydrogen expulsion can hardly compete with the elimination of a methyl radical. These thermochemical considerations are in good qualitative agreement with the observed intensities in the $^{-}$NIDD^{+} mass spectrum of **4**$^{-}$, displaying a small positive signal for $(CH_3)_2CO^{+\bullet}$ and a large peak for $CH_3CHO^{+\bullet}$. In contrast, losses of methane and ethane, which are formed from **4**$^{+}$ in formal 1,1-elimination processes, bear negative intensities in the difference spectrum. Labeling experiments show that the expulsion of methane from **4**$^{+}$ is a genuine 1,1-elimination, that is, there are large, negative signals for losses of CH_3D and CHD_3 from **4a**$^{-}$ and **4b**$^{-}$, respectively. The homologous *t*-butoxy radical **5**$^{\bullet}$ expels $CH_3^{\bullet}$ exclusively (Figure 4c). From the $^{-}$NIDD^{+} spectrum of **5a**$^{-}$ the secondary kinetic isotope effect for the elimination of $^{\bullet}CH_3$ versus $^{\bullet}CD_3$ can be estimated to be $k_{CH3}:k_{CD3} = 1.2$. The formation of acetyl ions by 1,1-elimination can be established by an examination of labeled **5b**$^{-}$. In the $^{-}$NIDD^{+} mass spectrum of **5b**$^{-}$ the signal for the acetyl ions is shifted to $m/z = 46$, which indicates that three deuterium atoms are present in this ionic fragment. If propyl ions are formed instead, they should incorporate seven deuterium atoms ($m/z = 50$); however, only a small peak is observed at this mass-to-charge ratio.

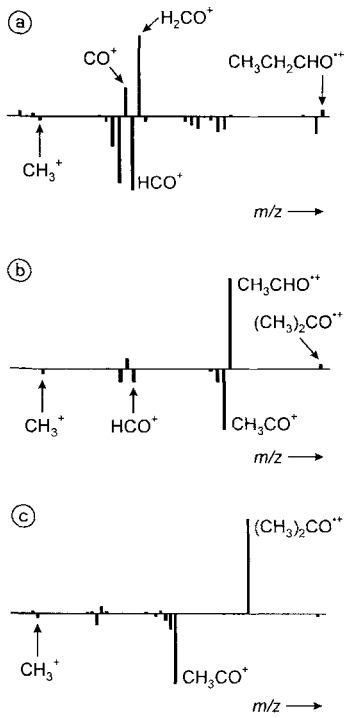

Figure 4. a) $^{-}$NIDD^{+} spectrum of *n*-propoxide ions **3**$^{-}$, b) $^{-}$NIDD^{+} spectrum of *i*-propoxide ions **4**$^{-}$, and c) $^{-}$NIDD^{+} spectrum of *t*-butoxide ions **5**$^{-}$.

In conclusion, $^{-}$NIDD^{+} is well suited for the investigation of the reactivity of neutral alkoxy radicals. A general reaction

  0947-6539/97/0311-1871 $ 17.50+.50/0

scheme evolves for radicals with short or branched side chains in that they lead to the carbonyl compounds by competing α-cleavages (Scheme 2). If the carbon adjacent to the radical center is substituted with different alkyl groups, a competition between different reaction channels is observed, depending on the thermochemical stabilities of the carbonyl compounds and the radicals formed during these processes. Last but not least, since similar results have been observed for alkoxy radical reactivities with entirely different experimental approaches,[4, 15] the difference method seems suitable to probe the reactivity of gaseous alkoxy radicals.

Barton-type 1,5-hydrogen migrations in transient alkoxy radicals: A new situation is encountered for alkoxy radicals with a chain length of more than three carbon atoms. These radicals have already been found[1, 4, 5] to undergo Barton-type 1,5-hydrogen migrations from C(4) to the oxygen atom via six-membered transition structures,[4, 5] thus resulting in the activation of C–H bonds remote from the functional group.[33] A large number of mechanistically related gas-phase reactions of radical cations giving rise to distonic ions are known and have been reviewed earlier.[34] To our knowledge, however, rearrangements of neutral radicals have so far not been studied using the NR technique.

n-Butoxy radical: In Figure 5 the $^-NR^+$ and $^-CR^+$ mass spectra of **6**$^-$ are displayed together with the corresponding difference spectrum. Three salient features of these spectra should be pointed out: a) The recovery signals are weak in the $^-NR^+$ and $^-CR^+$ spectra. b) Fragments corresponding to radical decompositions according to Scheme 2 are observed, such as the α-cleavage leading to propyl radicals and, with weak intensity, formaldehyde, which upon reionization give positive signals in the $^-NIDD^+$ spectrum (Figure 5c). c) In addition, three signals indicate the occurrence of an intramolecular hydrogen transfer to the oxygen centered radical:[35] protonated formaldehyde ions show up as a positive signal in the difference spectrum, indicating the formation of $^•CH_2OH$ radicals from neutral **6**$^•$. This is further supported by the positive signal for the $C_3H_6^{•+}$ fragment, which is the counterpart to the loss of $^•CH_2OH$ from **6**$^•$. Finally, the loss of water indicates the occurrence of a double hydrogen transfer to oxygen. Conducting these experiments with labeled **6a**$^-$, the origin of the migrating hydrogen atom is uncovered. In the $^-NR^+$ mass spectrum of **6a**$^-$, CH_2OD^+ and $[D_2]$propene cations are observed, the former clearly in line with a six-membered transition structure for a 1,5-hydrogen migration as observed in the Barton reaction.[11] However, the water loss is subject to partial H/D-exchange leading to a H_2O:HDO:D_2O ratio of ca. 1:10:5.

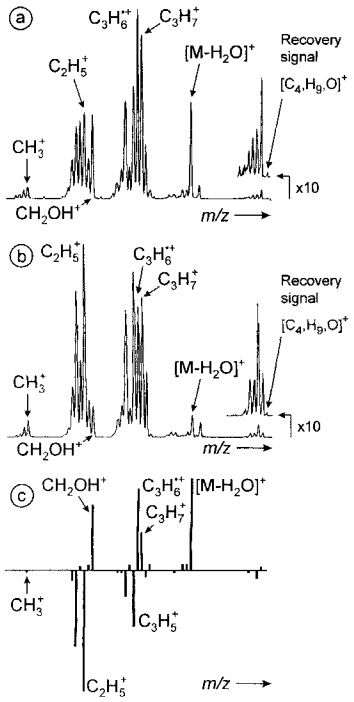

Figure 5. a) $^-NR^+$ mass spectrum (O_2, 80% T; O_2, 80% T), b) $^-CR^+$ mass spectrum (O_2, 80% T), and c) $^-NIDD^+$ spectrum of *n*-butoxide ions **6**$^-$.

n-Pentoxy radical: Compared with the *n*-butoxy system, the differences between charge reversal and neutralization–reionization mass spectra are more pronounced for the *n*-pentoxide ion (Figures 6a,b); hence, the $^-NIDD^+$ spectrum is also more instructive. Water loss as well as signals for the CH_2OH^+ cations and the complementary $C_4H_8^{•+}$ fragment are observed, which all give rise to positive signals in the difference mass spectrum (Figure 6c). In fact, the hydrogen-atom transfer to the oxygen-centered radical within the neutral is more pronounced compared to that in the C_4 system: while the signal for the water loss amounts to less than 15% of the base peak ($C_3H_5^+$) in the $^-CR^+$ mass spectrum (Figure 6b), it is the most abundant ion in the $^-NR^+$ experiment (Figure 6a). Products due to α-cleavages are not observed for **7**$^•$ as positive signals in the $^-NIDD^+$ spectrum.

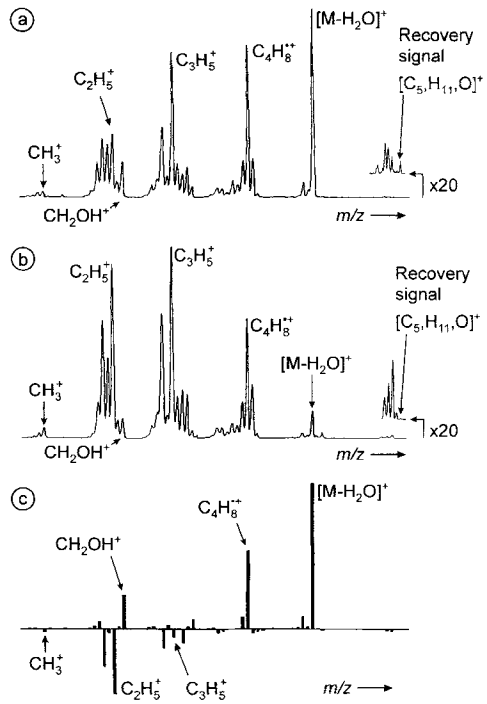

Figure 6. a) $^-NR^+$ mass spectrum (O_2, 80% T; O_2, 80% T), b) $^-CR^+$ mass spectrum (O_2, 80% T), and c) $^-NIDD^+$ spectrum of *n*-pentoxide ions **7**$^-$.

0947-6539/97/0311-1872 $ 17.50+.50/0 *Chem. Eur. J.* **1997**, *3*, No. 11

Owing to the fact that **7**• gave the most pronounced effects and that the products of the hydrogen migration are not masked by α-cleavages, we decided to study the $[C_5,H_{11},O]^•$ system in more detail by isotopic labeling experiments in conjunction with ab initio calculations. In order to exclude a conceivable hydrogen migration proceeding within the anion prior to neutralization, in the next sections we will first discuss the unimolecular and collision-induced fragmentation reactions of *n*-pentoxide ions $\mathbf{7}^-$. Then the neutralization process and the relevant parts of the potential energy surface for the neutral $[C_5,H_{11},O]^•$ isomers will be described, followed by a presentation of the cationic $[C_5,H_{11},O]^+$ potential energy surface.

Metastable alkoxide ions are known[36] to undergo dehydrogenation to yield enolates. The investigation of the labeled precursors $\mathbf{7a}^- - \mathbf{7e}^-$ provides a clear picture of this reaction. For $\mathbf{7c}^- - \mathbf{7e}^-$, which are labeled at positions remote from the oxygen atom, only elimination of H_2 is observed, while $\mathbf{7a}^-$ and $\mathbf{7b}^-$ decompose exclusively by expulsion of HD. The same result is obtained irrespective whether MI or CA mass spectra were recorded. No other processes are observed, most likely because electron loss sets an upper limit for the energy demands of these reactions. As demonstrated earlier,[36] the loss of molecular hydrogen from $\mathbf{7}^-$ leads to the corresponding enolate ion in a formal 1,2-elimination; this conjecture is fully in line with the isotopic labeling results. In marked contrast, the water loss in the $^-CR^+$ and $^-NR^+$ mass spectra of $\mathbf{7a}^-$ and $\mathbf{7b}^-$ is isotopically pure H_2O. Thus, these findings, together with the positive signals for $[M - H_2O]^+$ in the difference spectrum of $\mathbf{7}^-$ (Figure 6c) clearly demonstrate that the transfer of a hydrogen atom from the chain to the oxygen atom does not occur in the *n*-pentoxide ion. Rather, rearrangement is confined to a later stage, that is, to the neutral radical or the cation.

It is important to ensure that the neutralization step in the $^-NR^+$ experiments conducted with $\mathbf{7}^-$ yields predominantly the corresponding radical **7**• in the first step. This is indeed found experimentally, since the base peak in the $^-NR^-$ mass spectrum corresponds to reionized **7**• accompanied by a small signal for the $[\mathbf{7} - H_2]^-$ enolate ion (<10% of the recovery signal). Furthermore, the $^-CR^+$ mass spectrum of **7**• is rather insensitive to changes in the collision gas pressure. Therefore, the conditions outlined above for an application of the difference method are fulfilled. The resulting difference spectrum of unlabeled $\mathbf{7}^-$ is depicted in Figure 6c, and the spectra of the isotopomeric species $\mathbf{7a}^- - \mathbf{7e}^-$ in Figure 7.

In order to establish the course of the hydrogen-atom transfer, the experiments were carried out with isotopomers $\mathbf{7a}^- - \mathbf{7e}^-$. While the $^-NR^+$ and $^-CR^+$ mass spectra are rather complex, the mass shifts introduced by labeling can be analyzed quite easily in the difference spectra (Figure 7) as far as the positive components are concerned. Upon deuteration at C(1) (Figure 7a), formation of CD_2OH^+ concomitant with $C_4H_8^{•+}$ is found. This result supports the assumption that both fragments are due to the cleavage of the C(1)–C(2) bond in the neutral radical, followed by reionization. If this bond cleavage were to occur after reionization, on energetic grounds only an intense hydroxymethyl cation peak would be expected, following Stevenson's rule,[37] due to the different ionization energies of the fragments, IE(•CH_2OH) = 7.56 eV, IE(C_4H_8) > 9 eV.[24, 38] Analogously, all initial deuterium atoms are completely retained in the butene fragments for $\mathbf{7b}^-$, $\mathbf{7c}^-$, and $\mathbf{7e}^-$ (Figures 7b, c, e), demonstrating that only the C(4) position serves as the origin for the transferred hydrogen. This is further confirmed in that $\mathbf{7d}^-$ (Figure 7d) transfers one deuterium atom exclusively resulting, after reionization, in CH_2OD^+ and $C_4H_7D^{•+}$. From these findings, we conclude that the hydrogen-atom transfer in **7**• is regiospecific[39] and follows a Barton-analogous 1,5-hydrogen migration pattern, presumably involving a six-membered transition structure **TS7**•/**9**• (Scheme 3) without any competing H/D-exchange processes.

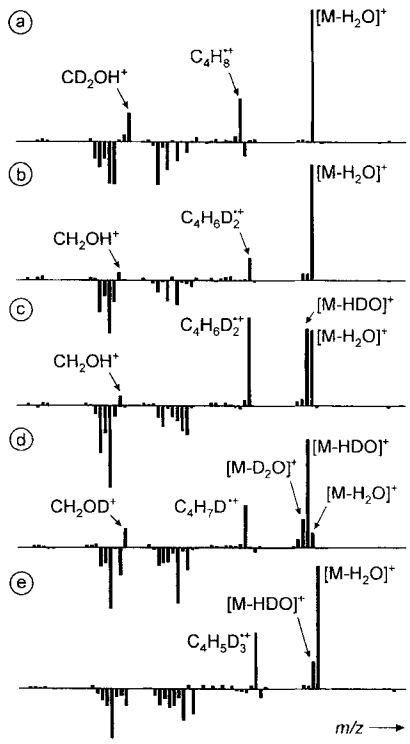

Figure 7. $^-NIDD^+$ spectra of a) [1,1-D_2]pentoxide $\mathbf{7a}^-$, b) [2,2-D_2]pentoxide $\mathbf{7b}^-$, c) [3,3-D_2]pentoxide $\mathbf{7c}^-$, d) [4,4-D_2]pentoxide $\mathbf{7d}^-$, and e) [5,5,5-D_3]-pentoxide ions $\mathbf{7e}^-$.

As far as the loss of water is concerned, the situation is somewhat more complicated, in that partial H/D-exchange is observed in the $^-NIDD^+$ mass spectra. Figures 7c–e demonstrate that mostly the hydrogen atoms originating from C(3)–C(5) of the hydrocarbon backbone contribute to this process. Owing to

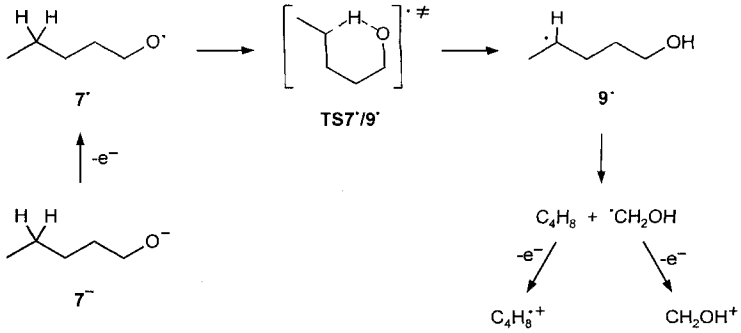

Scheme 3. Hydrogen-atom transfer in **7**• along a Barton-analogous 1,5-hydrogen migration pathway via a six-membered transition structure **TS7**•/**9**•.

  0947-6539/97/0311-1873 $ 17.50+.50/0

the fact that the first hydrogen transfer within the *n*-pentoxy radical is not subject to H/D-exchange (see above), the latter process must be associated with the migration of the second hydrogen to the hydroxyl group. On thermochemical grounds it is not reasonable to assume a second hydrogen transfer occurring within the neutral species. Instead, it is more plausible to argue that reionization to $\mathbf{9}^+$ precedes this migration. Following the mechanism depicted in Scheme 4, the second hydrogen transfer can be regarded as an intramolecular proton abstraction via a five-membered cyclic transition structure $\mathbf{TS9}^+/\mathbf{12}^+$ that leads to $\mathbf{12}^+$.[40] Furthermore, reionization of the carbon-centered radical $\mathbf{9}^\bullet$ to a carbenium ion can easily account for the experimentally observed partial H/D-exchange processes, if the proton transfer is reversible and facile Wagner–Meerwein rearrangements between $\mathbf{9}^+$ and $\mathbf{13}^+$ are assumed to be involved prior to the water loss. After isomerization of $\mathbf{9}^+$ to $\mathbf{13}^+$, intramolecular proton transfer via $\mathbf{TS13}^+/\mathbf{12}^+$ is possible. However, as will be shown below, the five-membered transition structure $\mathbf{TS9}^+/\mathbf{12}^+$ is quite favorable in energy. Thus, although the participation of $\mathbf{TS13}^+/\mathbf{12}^+$ cannot rigorously be excluded, this path was not pursued any further. A minor hydrogen exchange involves the C(5) position, as indicated by the positive $^-$NIDD$^+$ signal for loss of HDO in Figure 7e. Nevertheless, the H/D-exchanges can only be partial; this becomes clear from an inspection of Figures 7a and 7b, because the water loss shows no deuterium incorporation from the C(1) and C(2) positions. This would be expected if the Wagner–Meerwein processes within the alkyl chain were much faster than the expulsion of the H_2O moiety.

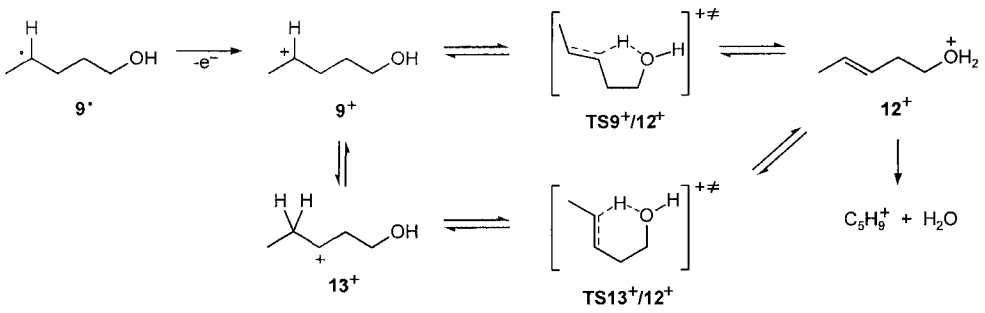

Scheme 4. Hydrogen transfers in **9** via cyclic transition states.

The water loss reveals an interesting aspect of the NIDD method. Although this process appears as a positive signal in the $^-$NIDD$^+$ spectrum of $\mathbf{7}^-$, it actually involves five individual steps: a) an initial hydrogen-atom transfer at the neutral stage to generate $\mathbf{9}^\bullet$, followed by b) a single electron transfer upon reionization, c) a subsequent proton migration, d) partial Wagner–Meerwein rearrangements, and e) loss of the water moiety. In other words, positive signals in the NIDD spectra need not necessarily represent processes which occur *exclusively* at the neutral stage; however, at least one of the reaction steps involved has to take place within the neutral intermediate. Therefore, this aspect has to be carefully considered in the interpretation of NIDD spectra.[41]

Often, the interpretation of mass spectral data is aided by the independent generation and investigation of ions of known connectivity. Comparison of the unimolecular and collision-induced fragmentations of a reference compound with the processes reflected in the difference spectra may thus provide additional support for the proposed mechanism for the H_2O loss. Therefore, we generated protonated 3-pentene-1-ol ($\mathbf{12}^+$) by chemical ionization of the neutral alcohol in a CH_5^+ plasma. The major reaction route in the MI and CA mass spectra of $\mathbf{12}^+$ is dehydration, in agreement with the proposal that $\mathbf{12}^+$ is an intermediate en route to the water loss.

Theoretical study of the n-pentoxy system: The experimental results for the $[C_5,H_{11},O]^{\bullet/+}$ systems are supported by extensive theoretical calculations performed at the Becke 3LYP/6-31G* level of theory. The relevant parts of the $[C_5,H_{11},O]^\bullet$ potential energy surface are depicted in Figure 8, the calculated energies of $[C_5,H_{11},O]^\bullet$ isomers and corresponding transition structures are listed in Table 3, and the corresponding optimized geometries of relevant species are depicted in Scheme 5. All fragment energies needed for the evaluation of the energetics of exit channels are given in Table 4.

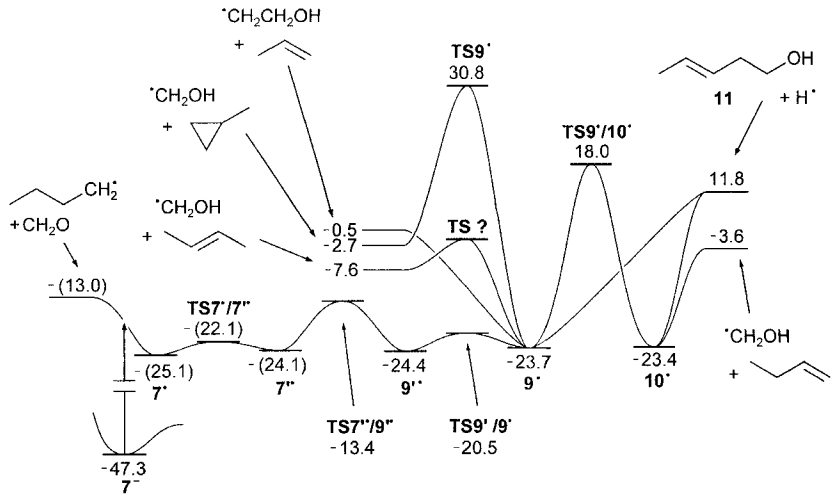

Figure 8. Calculated $[C_5,H_{11},O]^\bullet$ potential energy surface at the Becke 3LYP/6-31G* level of theory. The neutralization process $\mathbf{7}^- \rightarrow \mathbf{7}^\bullet$ is depicted as a vertical arrow. Note that the experimental energy demand[124] for the n-$C_3H_7^\bullet$ + CH_2O exit channel is ca. 5 kcal mol^{-1} higher than the calculated value (for details see Table 3 and text).

The extended structures $\mathbf{7}^-$ and $\mathbf{7}^\bullet$ are chosen as representatives for the whole variety of different conformers of unbranched $C_5H_{10}O^{\bullet/-}$; as shown in Scheme 5, the geometric differences between these two species are quite minor. As the

  0947-6539/97/0311-1874 $ 17.50+.50/0 *Chem. Eur. J.* **1997**, *3*, No. 11

Table 3. Calculated total energies (E_{total}), zero-point vibrational energies (ZPVE), and calculated as well as experimental heats of formation (ΔH_f) of $[C_5,H_{11},O]^{+\bullet}$ isomers and relevant fragmentation reactions.

	E_{total} (hartree) [a]	ZPVE (hartree)	ΔH_f (kcal mol^{-1}) [b]	ΔH_f (kcal mol^{-1}) [c]
7$^+$	−272.196193	0.150244	−47.3	−65 [d]
7$^\bullet$	−272.160739	0.151802	−25.1	−18.9
TS7$^\bullet$**/7**$''$	−272.156026	0.152228	−22.1	
7$''$	−272.159290	0.152286	−24.1	
TS7$''$**/9**$''$	−272.142100	0.147003	−13.4	
9$''$	−272.159690	0.152114	−24.4	
TS9$''$**/9**$^\bullet$	−272.153480	0.150961	−20.5	
9$^\bullet$	−272.158560	0.151210	−23.7	−23.9 [e]
TS9$^\bullet$**/10**$^\bullet$	−272.092098	0.147030	18.0	
10$^\bullet$	−272.158109	0.151473	−23.4	
TS9$^\bullet$	−272.073945	0.148196	30.8	
$CH_3CH_2CH_2CH_2^\bullet + H_2O$	−272.141536	0.144220	−13.0	−8.0
11 + H$^\bullet$	−272.101957	0.142118	11.8	10.0
$CH_3CH{=}CH_2 + {}^\bullet CH_2CH_2OH$	−272.121681	0.144704	−0.5	
trans-$CH_3CH{=}CHCH_3 + {}^\bullet CH_2OH$	−272.132907	0.146039	−7.6	−9.1
$CH_3CH_2CH{=}CH_2 + {}^\bullet CH_2OH$	−272.126587	0.146510	−3.6	−6.3
c-$C_3H_5CH_3 + {}^\bullet CH_2OH$	−272.116463	0.147586	−2.7	−0.7
$^3CH_3CH^\bullet CH_2CH_2^\bullet + {}^\bullet CH_2OH$	−272.031570	0.139679	56.0	

[a] Total energies based on Becke 3LYP/6-31G* optimized structures including ZPVE corrections (unscaled). [b] Calculated on the basis of literature data for the protonated 2-methyltetrahydrofuran, **14**$^+$ (see Computational Details). [c] Experimental data have been taken from ref. [24]. [d] Estimated on the basis of literature electron affinities for C_1–C_4 alkoxy radicals (see Computational Details and ref. [24]). [e] Estimated assuming BDE(RO–H) = 104 kcal mol^{-1} and BDE(C–H) = 99 kcal mol^{-1} for secondary alkyl C–H bonds (ref. [42]).

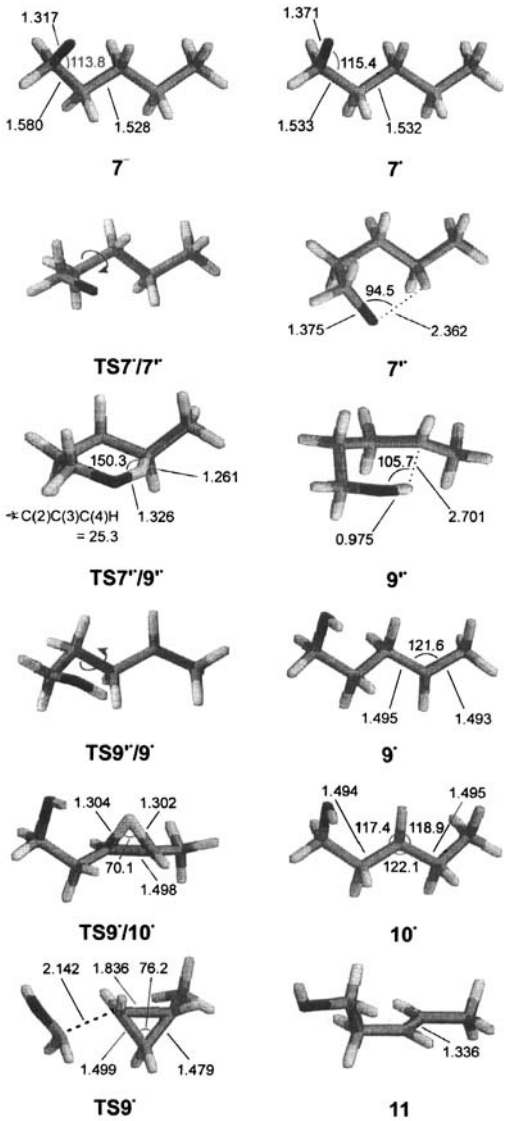

Scheme 5. Optimized geometries for species discussed in the text.

Table 4. Calculated total energies (E_{total}), zero-point vibrational energies (ZPVE), and experimental heats of formation (ΔH_f) of fragmentation products.

	E_{total} (hartree) [a]	ZPVE (hartree)	ΔH_f (kcal mol^{-1}) [b]
H$^\bullet$	−0.5002728	–	52.1
H_2O	−76.387794	0.021159	−57.8
CH_2O	−114.473657	0.026814	−26.0
$^\bullet CH_2OH$	−115.014517	0.037515	−6.2
$CH_3CH{=}CH_2$	−117.827487	0.080067	4.8
$^\bullet CH_2CH_2OH$	−154.294194	0.064637	
trans-$CH_3CH{=}CHCH_3$	−157.118390	0.108524	−2.9
$CH_3CH_2CH{=}CH_2$	−157.112070	0.108995	−0.1
c-C_3H_5–CH_3	−157.101946	0.110071	5.5
$^3CH_3CH^\bullet CH_2CH_2^\bullet$	−157.017053	0.102164	
$CH_3CH_2CH_2CH_2^\bullet$	−157.667879	0.117406	18.0
$CH_3CHCHCHCH_3^+$	−195.532002	0.124661	185.0
$CH_3CHCHCH_2CH_2OH$ (**11**)	−271.601684	0.142118	−42.0 [c]

[a] Total energies based on Becke 3LYP/6-31G* optimized structures including ZPVE corrections (unscaled). [b] Experimental data have been taken from ref. [24]. [c] Estimated on the basis of $\Delta H_f(CH_2{=}CHCH_2CH_2CH_2OH)$ = −41.0 kcal mol^{-1}, $\Delta H_f(CH_2{=}CH_2CH_2CH_2OH)$ = −36.0 kcal mol^{-1}, and $\Delta H_f(CH_3CH{=}CHCH_2OH)$ = −37.0 kcal mol^{-1} [24].

1,5-hydrogen migration does not proceed from **7**$^\bullet$, we searched first for the transition structure for rotation, **TS7**$^\bullet$**/7**$''$, to produce a conformer **7**$''$ which serves as a starting point for the Barton rearrangement. **TS7**$^\bullet$**/7**$''$ is located energetically ca. 3 kcal mol^{-1} above **7**$^\bullet$, and conformer **7**$''$ is 1 kcal mol^{-1} less stable than **7**$^\bullet$. The exit channel of lowest energy demand from **7**$^\bullet$ corresponds to the α-cleavage to generate *n*-$C_4H_9^\bullet$ and CH_2O, as discussed above (Scheme 1). Note that the calculated energy is ca. 5 kcal mol^{-1} lower than the experimental numbers.[24] This reaction defines an upper limit for the energy demand of any conceivable unimolecular rearrangement of $C_5H_{10}O^\bullet$. Thus, the transition structure **TS7**$''$**/9**$''$ for the Barton reaction must be located below this threshold. Indeed, **TS7**$''$**/9**$''$ fulfills this requirement, and the barrier height amounts to ≈11 kcal mol^{-1}, in fair agreement with literature data.[43] In a previous study,[5] the geometry of similar transition structures for the 1,5-hydrogen transfer in 2-hexoxy radicals has been dis-

  0947-6539/97/0311-1875 $ 17.50+.50/0

cussed based on force-field calculations. In line with earlier arguments,[14, 44] these authors proposed that the C(4)–H–O subunit is expected to be almost linear. For **TS7'•/9'•**, the geometry optimized at the Becke 3LYP/6-31G* level of theory gives a chairlike transition structure, where the C(4)–H–O bond is only slightly bent with ∢C(4)HO = 150.3°; relevant bond lengths are r(C(4)–H) = 1.261 and r(H–O) = 1.326 Å. The ∢C(2)C(3)C(4)H dihedral angle is only 25.3° instead of 60°, which is expected for a perfect chair conformation. The calculated transition structure can be interpreted as a compromise between a favorable chairlike conformation and minimized antibonding interactions between the unpaired radical electron and the C–H bond as realized in a quasilinear C-H-O subunit. The hydrogen migration product **9'•** can undergo rotation along the C(2)–C(3) bond to give rise to conformer **9•** with an extended hydrocarbon backbone. The calculated heat of formation of **9•** is slightly higher than that for **7•**, while widely accepted literature data[42] suggest that the bond dissociation energy of the O–H bond is about 5 kcal mol^{-1} higher than that of a secondary C–H bond. However, these differences are within the error limits of the theoretical approach.

Concerning the energetics of possible exit channels for **9•**, several pathways can be ruled out because these are much too high in energy compared with the $C_4H_9^+ + CH_2O$ exit channel from **7•**: a) Loss of a hydrogen atom from **9•** yielding 3-pentene-1-ol (**11**) is about 25 kcal mol^{-1} higher in energy than the threshold. Indeed, this channel is not observed experimentally. b) Cleavage of the C(2)–C(3) bond leads to propene and a $^{\bullet}CH_2CH_2OH$ radical, and a very minor positive signal is observed for the cation in the $^-$NIDD$^+$ mass spectrum of **7•**. c) As far as the formation of C_4H_8 is concerned, several isomers are conceivable. Simple bond cleavage of the C(1)–C(2) bond in **9•** yielding a 1,3-butadiyl biradical in its triplet state needs ca. 80 kcal mol^{-1} and is not feasible. A transition structure **TS9•** for the formation of methylcyclopropane by backside attack of the C(4) centered radical at C(2) with $^{\bullet}CH_2OH$ as a leaving group could be located. However, with an energy demand of more than 50 kcal mol^{-1}, this path is far outside the energy regime and can thus be ruled out. Formation of 1-butene together with $^{\bullet}CH_2OH$ radicals appears as an alternative, but the isomerization of **9•** to **10•** by a 1,2-hydrogen shift (**TS9•/10•**), which necessarily has to precede this type of C(1)–C(2) bond cleavage, is too high in energy. Assuming that the literature heat of formation of −8.0 kcal mol^{-1} for the $C_4H_9^+ + CH_2O$ exit channel and the one for the $^{\bullet}CH_2OH$ radical (−6.2 kcal mol^{-1}) are correct, no C_4H_8 isomers with heats of formation of more than −1.8 kcal mol^{-1} are likely to be formed. Thus, only *cis*- and *trans*-2-butene (−1.9 and −2.9 kcal mol^{-1}, respectively)[24] or 2-methyl propene (−4.0 kcal mol^{-1}) represent possible reaction products. Formation of the latter needs extensive rearrangement of the hydrocarbon backbone, which is not very likely to occur. Therefore, we tried to optimize a transition structure for the cleavage of the C(1)–C(2) bond of **9•**, coupled with a concerted, radical-assisted 1,2-hydrogen migration from C(3) to C(2). This reaction would give rise to *trans*- or *cis*-2-butene and $^{\bullet}CH_2OH$. However, we unfortunately did not succeed in localizing this TS and the quest for the exact mechanism for the fragmentation step yielding C_4H_8 and $^{\bullet}CH_2OH$ remains uncompleted.[45]

Part of the $[C_5,H_{11},O]^+$ potential energy surface (Figure 9) can already be constructed from energetic data (Table 5) for several isomers and transition structures (Scheme 6) relevant for a rationalization of the water loss. The starting point is the

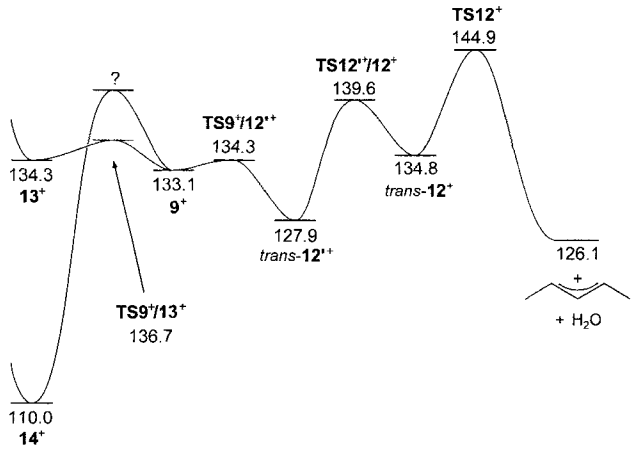

Figure 9. Part of the calculated $[C_5,H_{11},O]^+$ potential energy surface relevant for the water loss at the Becke 3LYP/6-31G* level of theory.

Table 5. Calculated total energies (E_{tot}), zero-point vibrational energies (ZPVE), and calculated as well as experimental heats of formation (ΔH_f) of $[C_5,H_{11},O]^+$ isomers and relevant fragmentation reactions.

	E_{tot} (hartree) [a]	ZPVE (hartree)	ΔH_f (kcal mol^{-1}) [b]	ΔH_f (kcal mol^{-1}) [c]
9$^+$	−271.908699	0.151700	133.1	
TS9$^+$/12'$^+$	−271.906776	0.149739	134.3	
***trans*-12'$^+$**	−271.916990	0.154839	127.9	
TS12'$^+$/12$^+$	−271.898304	0.154271	139.6	
***trans*-12$^+$**	−271.906007	0.154060	134.8	
***cis*-12'$^+$**	−271.913942	0.155070	129.8	
***cis*-12$^+$**	−271.903386	0.154378	136.4	
TS12$^+$	−271.888717	0.147004	144.9	
13$^+$	−271.906859	0.151430	134.3	
TS9$^+$/13$^+$	−271.902932	0.150930	136.7	
14$^+$	−271.945512	0.158183	110.0	110.0 [b]
15$^+$	−271.933449	0.155413	117.6	118.0
^{3}7$^+$	−271.823780	0.148624	186.4	
^{3}15$^+$	−271.811232	0.147812	194.3	
TS^{3}7$^+$/^{3}15$^+$	−271.761287	0.143567	225.6	
$CH_3CH{=}CHCH_3{\cdot}H_2O$	−271.919796	0.145820	126.1	127.2

[a] Total energies based on Becke 3LYP/6-31G* optimized structures including ZPVE corrections (unscaled). [b] Calculated on the basis of literature data for the protonated 2-methyltetrahydrofuran, **14$^+$** (see Computational Details). [c] Experimental data have been taken from ref. [24].

reionized species **9$^+$**. In addition to the reactions depicted in Scheme 4 several other rearrangements are feasible: a) Ring closure by attack of one of the nucleophilic lone pairs of the oxygen atom at C(4) leads to protonated 2-methyltetrahydrofuran (**14$^+$**), which is more stable than **9$^+$** by ca. 23 kcal mol^{-1}. As **9$^+$** and **14$^+$** were characterized as genuine minima, one would expect to see a transition structure connecting both. However, several attempts to locate **TS9$^+$/14$^+$** failed. Although

0947-6539/97/0311-1876 $ 17.50+.50/0 Chem. Eur. J. 1997, 3, No. 11

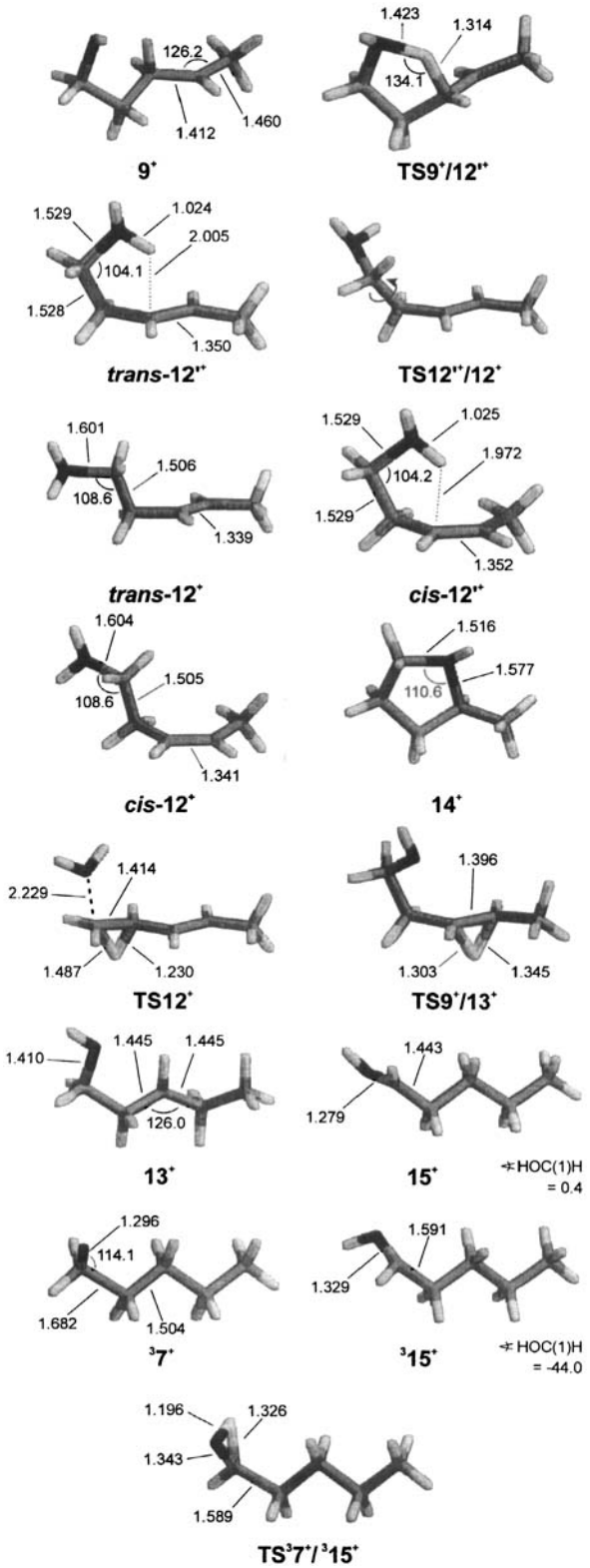

Scheme 6. Optimized geometries for species discussed in the text.

the energy demand for ring closure is not known, it is expected to be rather low. This is also indicated by MI experiments with independently generated protonated methyltetrahydrofuran, which expels only water upon unimolecular decay. This process points to a rather facile ring-opening reaction. b) In contrast to anions[46] or radicals, secondary carbenium ions such as $\mathbf{9}^+$ are expected to undergo facile interconversion with $\mathbf{13}^+$ (Scheme 4).[47] This is supported by the calculations. The species $\mathbf{9}^+$ and $\mathbf{13}^+$ are more or less isoenergetic, with heats of formations of 133.1 and 134.3 kcal mol^{-1}, respectively. The transition structure $\mathbf{TS9}^+/\mathbf{13}^+$, which connects the two carbenium ions, is located only 3.6 kcal mol^{-1} above $\mathbf{9}^+$, but clearly below the transition structure $\mathbf{TS12}^+$ leading to the water loss. Hence, as observed experimentally, H/D-exchanges invoking C(3)/C(4) are easily accessible. c) Surprisingly, the barrier $\mathbf{TS9}^+/\mathbf{12'}^+$ describing the intramolecular proton abstraction (Scheme 4) is located only ca. 1 kcal mol^{-1} above $\mathbf{9}^+$. It is connected with protonated *trans*-3-pentene-1-ol (*trans*-$\mathbf{12'}^+$), which is stabilized in its bent conformation owing to interactions of the double bond with one of the acidic hydrogens at the oxygen atom (Scheme 6).[10j] This becomes clear when considering a rotation around the C(1)–C(2) bond ($\mathbf{TS12'}^+/\mathbf{12}^+$) leading to the extended hydrocarbon side chain in *trans*-$\mathbf{12}^+$. Conformer $\mathbf{12}^+$ is higher in energy than $\mathbf{12'}^+$ by ca. 7 kcal mol^{-1} and even higher than $\mathbf{TS9}^+/\mathbf{12'}^+$. For comparison, the corresponding *cis* isomers were also optimized; they were found to be located above their *trans*-configurated analogues by $\approx$1.5 to 2 kcal mol^{-1}. Finally, the water loss most probably does not proceed stepwise with a primary 3-pentene-1-yl cation as intermediate, since this cation is not expected to exist as a minimum on the $[C_5,H_9]^+$ potential energy surface.[48] Instead, we succeeded in locating a transition structure $\mathbf{TS12}^+$ for a concerted water loss combined with a 1,2-migration of one of the C(2) hydrogen atoms to C(1) yielding the energetically favorable 1,3-dimethylallyl cation as ionic product. $\mathbf{TS12}^+$ is located $\approx$12 kcal mol^{-1} above reionized $\mathbf{9}^+$ and is higher in energy as compared to $\mathbf{TS9}^+/\mathbf{12'}^+$ and $\mathbf{TS12'}^+/\mathbf{12}^+$.

Nevertheless, the computed potential energy surface does not satisfactorily explain the experimental H/D-distribution observed for the water loss. As $\mathbf{TS9}^+/\mathbf{12'}^+$ is located more than 10 kcal mol^{-1} below $\mathbf{TS12}^+$, the intramolecular proton transfer proposed in Scheme 4 is reversible. Furthermore, the 1,2-proton shift $\mathbf{9}^+ \rightarrow \mathbf{13}^+$ can easily compete with the water loss due to the low energy demand of $\mathbf{TS9}^+/\mathbf{13}^+$. Thus, from the calculated $[C_5,H_{11},O]^+$ potential energy surface, one expects a more complete H/D-equilibration prior to the water loss, in particular also participation of the hydrogen atoms at C(1) and C(2). This is not in perfect agreement with the isotope pattern for the water losses observed in the $^-NR^+$ mass spectra of $\mathbf{7a}^- - \mathbf{7e}^-$. Note that the water loss from $\mathbf{12}^+$ could also be described in terms of an ion-dipole mechanism.[49] Nevertheless, for this mechanistic alternative too an activation of the C–H bonds at C(1) and C(2) would be expected. This is not observed in the experiments (Figure 7a and 7b). Therefore, this aspect remains open to further investigation and will not be pursued further.

Furthermore, the computational study explains why the $^-NR^+$ spectra do not exhibit an intense survivor signal, although $\mathbf{9}^+$ or $\mathbf{13}^+$ represent stable cations: single-point calculations of $\mathbf{9}^\bullet$ and $\mathbf{9}^+$ at the equilibrium geometry of the neutral yield a vertical ionization energy of $\mathbf{9}^\bullet$ of $\approx$173 kcal mol^{-1}; this number is about 15 kcal mol^{-1} larger than the adiabatic IE. Thus, most of the $\mathbf{9}^+$ ions generated during the reionization step contain enough internal energy to surmount the barrier for the water loss, and only very few ions exhibit lifetimes long enough to give rise to the recovery signals in the NR spectra.

As already stated, it is known from the methoxy system that triplet alkoxy cations can be generated by charge inversion of the anions.[27, 28] Therefore, some exploratory calculations were performed for the $^3[C_5,H_{11},O]^+$ potential energy surface. While all attempts to locate a singlet pentoxy cation failed and geometry optimization always resulted in protonated pentanal ($\mathbf{15}^+$) the triplet pentoxy cation $^3\mathbf{7}^+$ was found to be a stable species. However, it is located energetically far above the singlet potential energy surface; for example, the energy difference between $\mathbf{9}^+$ and $^3\mathbf{7}^+$ amounts to more than 53 kcal mol^{-1}. Similarly, $^3\mathbf{15}^+$ is higher in energy than its singlet analogue $\mathbf{15}^+$ by as much as $\approx$77 kcal mol^{-1}. In addition, the transition structure $\mathbf{TS}^3\mathbf{7}^+/^3\mathbf{15}^+$ has been localized; both $^3\mathbf{15}^+$ and $\mathbf{TS}^3\mathbf{7}^+/^3\mathbf{15}^+$ are found to be even higher in energy than $^3\mathbf{7}^+$. In principle, $^3\mathbf{7}^+$ bears radicaloid character and would, therefore, be expected to exhibit a similar reactivity to that of neutral $\mathbf{7}^\bullet$. Consequently, the differences between the $^-NR^+$ and $^-CR^+$ mass spectra might be due to formation of $^3\mathbf{7}^+$ with different internal energy content. In order to ensure that the positive signals in the $^-NIDD^+$ spectra are indeed due to the reactivity of neutrals, we performed single-point calculations for $^3\mathbf{7}^+$ at the geometries of $\mathbf{7}^\bullet$ and $\mathbf{7}^-$ as a qualitative measure for the amount of excess energy stored in $^3\mathbf{7}^+$ formed by either $^-NR^+$ or $^-CR^+$ experiments. One-electron oxidation of neutral $\mathbf{7}^\bullet$ leads to triplet pentoxy cations with ca. 8 kcal mol^{-1}, while two-electron oxidation of $\mathbf{7}^-$ gives rise to $^3\mathbf{7}^+$ with ca. 11 kcal mol^{-1} excess internal energy. Although it is not impossible that $^3\mathbf{7}^+$ is formed in the $^-CR^+$ or $^-NR^+$ experiments, the positive signals in the $^-NIDD^+$ spectra are not likely to originate from these species, because the difference in internal energy is rather small.

There is one additional aspect which has to be pointed out. Once $\mathbf{7}^\bullet$ is formed by neutralization of $\mathbf{7}^-$, two competing reaction pathways are accessible: direct bond cleavage to yield CH_2O together with n-$C_4H_9^\bullet$, and hydrogen-atom transfer to give rise to the Barton product. According to the calculations, both processes have the same energy demand, so the bond cleavage should be entropically favored over the hydrogen migration. Nevertheless, the experiments reveal a preference for the rearrangement pathway. This can be attributed to the fact that the calculated $CH_2O + n$-$C_4H_9^\bullet$ exit channel is underestimated by ca. 5 kcal mol^{-1} compared to the literature data,[24] while the calculated energy demand for $\mathbf{TS7}'^\bullet/\mathbf{9}'^\bullet$ is at the upper limit of the data given in the literature.[43] Besides this limitation, the experimental and theoretical results are reasonably consistent.

Finally, let us address the differences in the $^-NIDD^+$ spectra of $\mathbf{6}^\bullet$ and $\mathbf{7}^\bullet$. Although the mechanistic features of the 1,5-hydrogen migration in n-butoxy radicals $\mathbf{6}^\bullet$ are expected to be similar to that of $\mathbf{7}^\bullet$, the thermochemistry differs slightly. While the energetics of the α-cleavage reaction to give rise to CH_2O and $R^\bullet$ is comparable[24] for $C_4H_9O^\bullet$ ($\mathbf{6}^\bullet$) and $C_5H_{11}O^\bullet$ ($\mathbf{7}^\bullet$), this is not the case for the initial product of the Barton rearrangement: $\mathbf{6}^\bullet$ gives rise to a primary carbon-centered radical, while the more stable secondary radical $\mathbf{9}^\bullet$ is formed from $\mathbf{7}^\bullet$.

Diastereoselectivity of the 1,5-hydrogen transfer in neutral 3-methylpentoxy radicals: In the last section of this study, stereochemical features of the 1,5-hydrogen migration in alkoxy radicals should be tackled. To this end, we introduced a methyl group at the C(3) position of a pentoxy radical as a stereochemical marker. As will be shown, the stereoselectivity of the hydrogen migration can be monitored using the diastereospecifically labeled [4-D_1]3-methylpentoxy radicals $\mathbf{8e}^\bullet$ and $\mathbf{8f}^\bullet$, while the regiochemistry is assessed with $\mathbf{8a}^\bullet$–$\mathbf{8d}^\bullet$.

Typically, mass spectra of stereoisomers differ in only a few, structurally significant fragmentations,[50, 51] while most of the observed dissociations yield little or no stereochemical information. The same applies to the fragmentations observed in the $^-NR^+$ and $^-CR^+$ spectra of $\mathbf{8}^-$ (Figure 10) and its isotopomers, and we will refrain from discussing in detail the rich chemistry which these species exhibit upon neutralization–reionization or charge reversal to cations. Rather, we will focus on those processes which are relevant for the elucidation of the diastereoselectivity in the 1,5-hydrogen-atom transfer in the neutral alkoxy radicals.

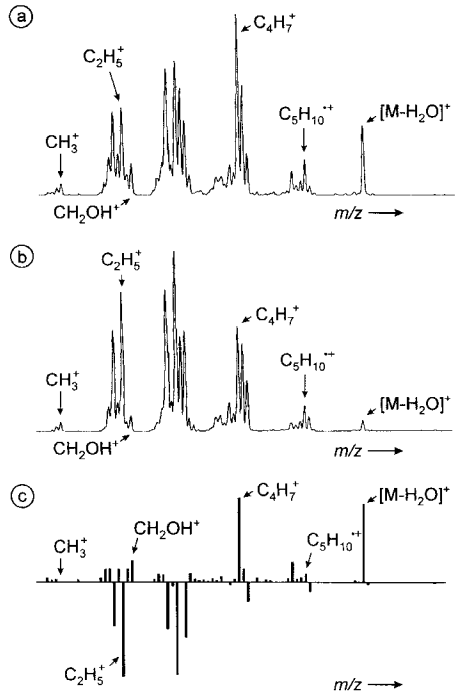

Figure 10. a) NR mass spectrum (O_2, 80% T; O_2, 80% T), b) CR mass spectrum (O_2, 80% T), c) difference mass spectrum of *rac*-3-methylpentoxide ion $\mathbf{8}^-$.

In analogy to the n-pentoxy system, the $^-NIDD^+$ spectrum of $\mathbf{8}^-$ (Figure 10c) shows two particular features which indicate a hydrogen-atom transfer from the alkyl chain to the oxygen-centered radical: a) A fragment corresponding to the hydroxymethyl cation CH_2OH^+ ($m/z = 31$) appears as a positive signal in the difference spectrum and points towards O–H bond formation in the neutral radical. Note that the corresponding counterpart $C_5H_{10}^{+\bullet}$ does also give rise to a positive signal together with the characteristic $C_4H_7^+$ fragment. b) Similarly, the positive signal for loss of water ($\Delta m = 18$) can only be accounted for by a double hydrogen transfer to oxygen. However, for the discussion of the regio- and diastereoselectivity associated with the hydrogen-atom transfer only the formation of the hydroxymethyl cation is instructive. As for $\mathbf{7}^\bullet$, water loss from $\mathbf{8}^\bullet$ is associated with partial hydrogen exchange; for example, for the

0947-6539/97/0311-1878 $ 17.50+.50/0 *Chem. Eur. J.* **1997**, *3*, No. 11

isotopomer $\mathbf{8b}^-$, a ratio for H_2O:HDO:D_2O loss of 1.1:2.9:1.0 is observed in the difference spectrum. In addition, formation of $C_5H_{10}^{\bullet+}$, the counterpart of CH_2OH^+, suffers from isobaric interferences by alkyl fragments formed at the ionic stage.

Prior to the discussion of stereochemical effects, the site selectivity involved in the formation of CH_2OH^+ needs to be elaborated. In contrast to the *n*-pentoxy radical, model system **8** has two sites that are in principle suitable for a 1,5-hydrogen-atom transfer. To this end the $^-NR^+$ and the $^-CR^+$ spectra of the isotopomers $\mathbf{8a}^-$–$\mathbf{8d}^-$ were recorded and the corresponding difference spectra derived. In particular for the alkoxides $\mathbf{8c}^-$–$\mathbf{8d}^-$, multiple labeling was essential to avoid isobaric interferences. Upon deuteration at C(1), positive signals for CD_2OH^+ ($m/z = 33$) in conjunction with its congener $C_5H_{10}^{\bullet+}$ are observed in the difference spectrum of the isotopomer $\mathbf{8a}^-$. This finding indicates that both fragments are formed by cleavage of the C(1)–C(2) bond on the neutral stage followed by reionization. The origin of the transferred hydrogen atom is clearly revealed by the signals for CD_2OH^+ versus CD_2OD^+ in the difference spectra of the labeled precursors $\mathbf{8b}^-$–$\mathbf{8d}^-$ (Table 6). For example, $\mathbf{8b}^-$ leads to the formation of 16% CD_2OH^+ and 84% CD_2OD^+, whereas in the difference spectrum of $\mathbf{8c}^-$ 88% CD_2OH^+ and 12% CD_2OD^+ are observed. These results undoubtedly reflect the preference of the oxygen-centered radical to abstract a hydrogen atom from the secondary C–H bond of the C(4) position as compared to the cleavage of a primary C–H bond from the methyl group attached at C(3). While both processes represent 1,5-hydrogen migrations, the latter results in an energetically less favorable primary carbon-centered radical **17**• (Scheme 7). Accordingly, the isotopomer $\mathbf{8d}^-$ displays a very small signal (3%) for CD_2OD^+ in conjunction with a large signal (97%) for CD_2OH^+, thus indicating that hydrogen-atom transfer from the C(5) position is negligible. From these findings, we conclude that the hydrogen-atom migration proceeds preferentially by a 1,5-hydrogen transfer mechanism involving the C(4) position, and to a first approximation[52] the branching ratio amounts to 86:14 (Scheme 7).

Table 6. Normalized data for the intensities of hydroxymethyl cations in the difference spectra of isotopomeric 3-methylpentoxide ions ($\mathbf{8a}^-$–$\mathbf{8f}^-$) [a].

Precursor	CH_2OH^+	CH_2OD^+	CD_2OH^+	CD_2OD^+
$\mathbf{8a}^-$	–	–	100	0
$\mathbf{8b}^-$	–	–	16	84
$\mathbf{8c}^-$	–	–	88	12
$\mathbf{8d}^-$	–	–	97	3
$\mathbf{8e}^-$	87 [b]	13 [b]	–	–
$\mathbf{8f}^-$	33 [b]	67 [b]	–	–

[a] Intensities are normalized to the sum of hydroxymethyl loss = 100%. [b] Reported intensities are the average of several independent measurements, and the error bars do not exceed 10%.

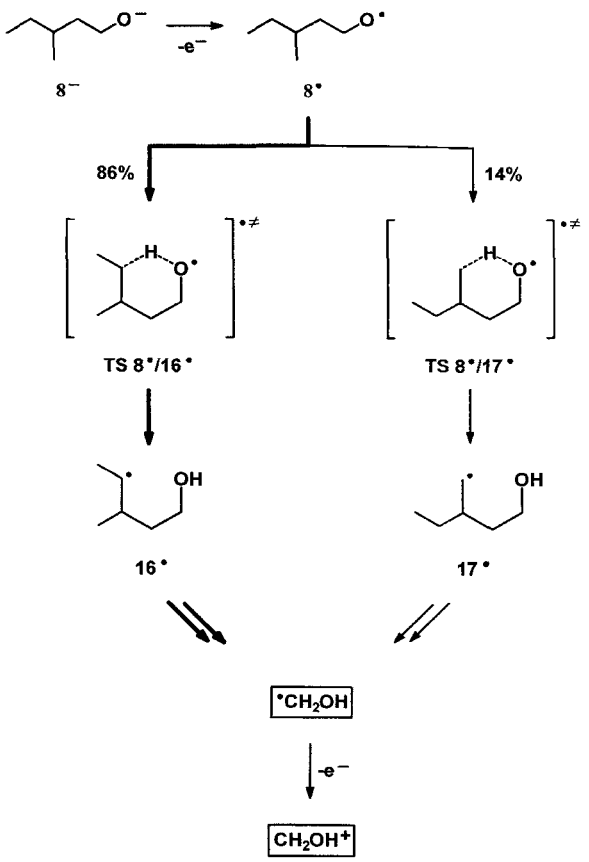

Scheme 7. 1,5-hydrogen migrations from the oxygen-centered radical **8**•; the cleavage of a primary C–H bond from the methyl group at C(3) results in an energetically less favorable primary carbon-centered radical **17**• than abstraction of a hydrogen atom from the secondary C–H bond of the C(4) position.

In the following discussion of the diastereoselectivity of the 1,5-hydrogen migration we neglect the small contribution of the path proceeding via **TS8•/17•**, which—as will be shown—does not affect our analysis of the observed diastereoselective discrimination. Hence, the diastereoselectivity can be assessed by comparing the intensities of the CH_2OH^+ and CH_2OD^+ fragments arising from the diastereoisomers, that is, the alkoxy radicals $\mathbf{8e}^•$ and $\mathbf{8f}^•$. Note that these fragments are not subject to isobaric interference from alkyl fragments. The $^-NIDD^+$ spectra (Figures 11 and 12) demonstrate that the ratio of CH_2OH^+ versus CH_2OD^+ formation is significantly larger for the isotopomer $\mathbf{8e}^-$ (6.4:1) than for its diastereoisomer $\mathbf{8f}^-$ (0.5:1). As the only difference between the anions $\mathbf{8e}^-$ and $\mathbf{8f}^-$ is the relative stereochemistry at the C(3) position, the striking diastereoselectivity has to be traced back to the transition structures in the course of the 1,5-hydrogen (deuterium) migration.

Of course, in addition to a stereochemical effect (SE), the measured CH_2OH^+/CH_2OD^+ ratios for $\mathbf{8e}^-$ and $\mathbf{8f}^-$ are also affected by the operation of a kinetic isotope effect (KIE). Assuming the combined action of a steric and a kinetic effect, it is possible to estimate semiquantitatively the magnitude of these two effects by applying a simple algebraic approach.[12d, 51] The measured intensities of CH_2OH^+ and CH_2OD^+ allow the determination of the two relevant components as KIE $= 1.8 \pm 0.3$ and SE $= 3.6 \pm 1.3$ for the 1,5-hydrogen-atom transfer in neutral 3-methylpentoxy radicals.[53, 54]

A straightforward analysis of these experimental results can be accomplished on the basis of the idealized mechanistic scenario depicted in Scheme 8 for the diastereoisomer $\mathbf{8e}^-$.[55] Upon electron detachment from the anion $\mathbf{8e}^-$ the neutral radical $\mathbf{8e}^•$ is formed, which can subsequently adopt conformations with suitable geometries for the 1,5-hydrogen (deuterium) transfer involving C(4). Thus, two chairlike conformations are pos-

  0947-6539/97/0311-1879 $ 17.50+.50/0

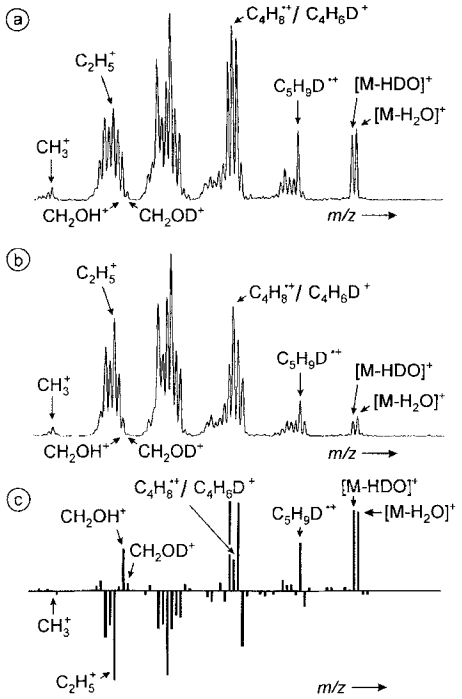

Figure 11. a) NR mass spectrum (O_2, 80% T; O_2, 80% T), b) CR mass spectrum (O_2, 80% T), c) difference mass spectrum of a diastereomerically pure mixture of *(3S, 4S)*-[4-D_1]- and *(3R, 4R)*-[4-D_1]3-methylpentoxide ions **8e**$^-$.

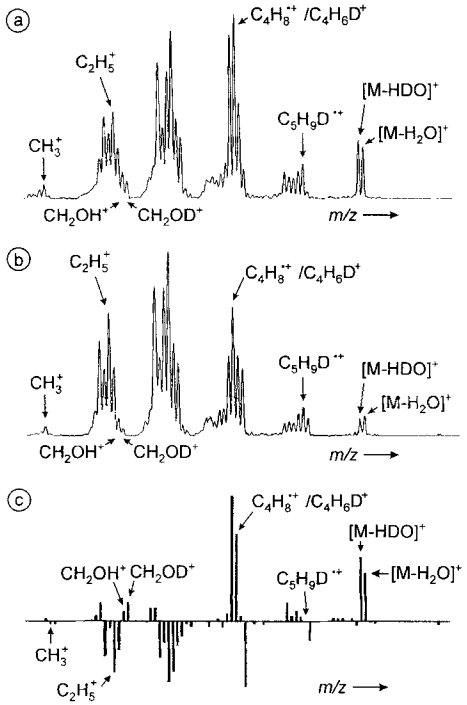

Figure 12. a) NR mass spectrum (O_2, 80% T; O_2, 80% T), b) CR mass spectrum (O_2, 80% T), c) difference mass spectrum of a diastereomerically pure mixture of *(3R, 4S)*-[4-D_1]- and *(3S, 4R)*-[4-D_1]3-methylpentoxide ions **8f**$^-$.

sible, **TS8e$^\bullet$/16e$^\bullet$** and **TS8e$^\bullet$/16e$''^\bullet$**, leading to H- and D-atom transfer, respectively. As a result, the carbon-centered radicals **16e$^\bullet$** and **16e$''^\bullet$** are formed, which subsequently decompose and, after reionization of the neutral hydroxymethyl fragments, yield the corresponding CH_2OH^+/CH_2OD^+ cations. For the diastereoisomer **8e$^\bullet$**, the geometry of the TS associated with migration

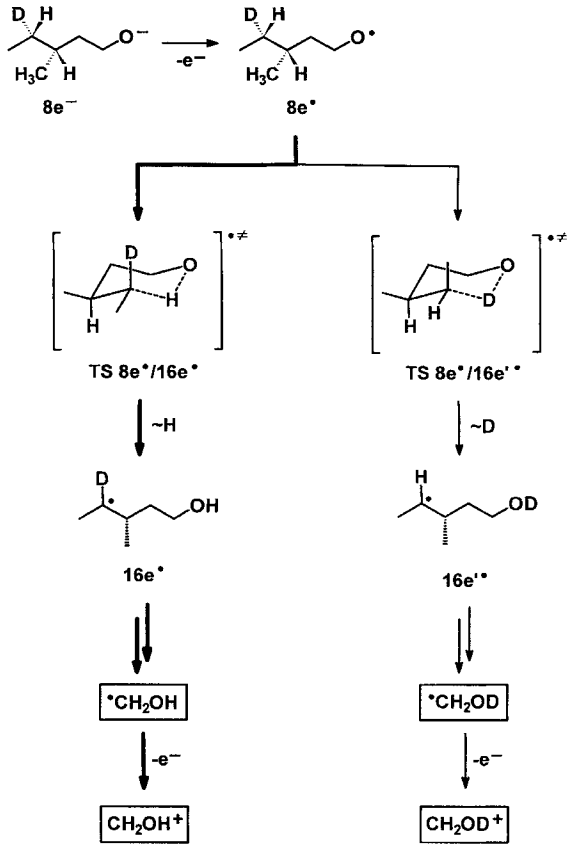

Scheme 8. Idealized mechanistic scenario for the diastereoisomer **8e**$^-$.

of a hydrogen atom is a chairlike structure in which both methyl substituents adopt favorable equatorial positions. In contrast, deuterium transfer from **8e$^\bullet$** has to proceed via **TS8e$^\bullet$/16e$''^\bullet$**, in which one of the methyl groups is forced into the energetically less favorable axial position.

However, the theoretical investigation of the *n*-pentoxy parent system has revealed that this model is idealized, in that it assumes a perfect chairlike transition structure for the 1,5-hydrogen migration, neglecting the partial linearization of the C(4)–H–O moiety (see above). The Newman-type representations depicted in Scheme 9 clarify the influence of this effect. For example, in **TS8e$^\bullet$/16e$^\bullet$** (corresponding to the migration of a hydrogen atom, Scheme 8) the 1,2-interactions of the two methyl groups at C(3) and C(4) are reduced upon linearization

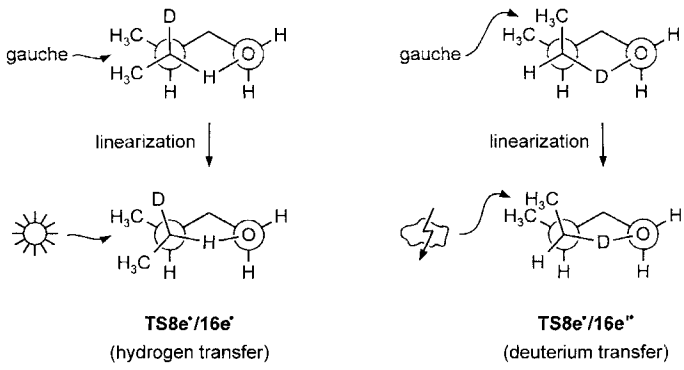

Scheme 9. Newman-type representations showing the partial linearization of the C(4)–H–O moiety in the *n*-pentoxy transition structure and its results.

0947-6539/97/0311-1880 $ 17.50+.50/0 *Chem. Eur. J.* **1997**, *3*, No. 11

of the C(4)–H–O subunit. In contrast, in **TS8e'/16e''** for the deuterium shift, these steric interactions are intensified compared to an ideal chairlike structure.

Both pictures, the conformational analysis of chairlike transition structures and the description in terms of 1,2-interactions of the methyl groups, predict that the isotopomer **8e'** will preferentially undergo hydrogen-atom transfer, because this path is favored by the reduced steric interaction as well as by the kinetic isotope effect, thus giving rise to a large CH_2OH^+/CH_2OD^+ ratio. In contrast, in the diastereoisomer **8f'** with an inverted relative stereochemistry at the C(3) position, deuterium-atom transfer will be conformationally favored, but kinetically hampered; consequently SE and KIE almost cancel out, as is indeed observed experimentally.

These findings are in qualitative agreement with previous studies of alkoxy radicals in the condensed phase. For example, Green et al.[5] examined the stereoselectivity and the kinetic isotope effect for the 1,5-hydrogen transfer reaction of 2-hexyloxy radicals in order to probe the transition structure for the Barton reaction. However, in contrast to the 3-methylpentoxy system studied in this contribution, a large kinetic isotope effect of the order of 6 at 25 °C and relatively little stereochemical discrimination (1.23:1) were found. These differences can easily be attributed to the different model compounds employed; the 3-methylpentoxy system is affected by 1,2-interactions, whereas in the case of the 2-hexyloxy radicals only 1,4-interactions are feasible; these are expected to be weaker. The kinetic isotope effect, however, is much larger in solution, as these experiments were performed at ambient temperature, while the internal energies of the transient radicals correspond to higher temperatures. In addition, radical reactions studied at a molecular level in the gas phase cannot directly be compared to analogous investigations performed in solution, in particular when the generation of polar groups (e.g. OH) is involved.[2]

Conclusions

Two distinct reactivity patterns arise for the alkoxy radicals presented in this study. Small neutral alkoxides react by α-cleavage to yield the corresponding carbonyl compounds. Alkoxy radicals with side chains bearing more than three carbon atoms give rise to Barton-type hydrogen migrations. This process has been studied in detail by experimental as well as theoretical means for *n*-pentoxy radicals, leading to a pleasing agreement of the gas-phase data with results obtained in condensed matter.

The application of the NIDD method to diastereoselectively labeled [4-D_1]3-methylpentoxy radicals demonstrates that, despite the high-energy collisions used to generate the neutrals, these species show distinct regio- and stereochemistry in the subsequent Barton-type reaction at the neutral stage.

In conclusion, it has been demonstrated that this new application of sector mass spectrometry provides direct insight into the chemistry of radicals at a molecular level. When this type of equipment is available, the experiments are readily performed; such mass spectrometry provides an alternative approach to examine the reactivity of radicals unperturbed by any intermolecular interactions. In addition, besides the investigation of the reactivity of neutral intermediates in the gas phase, this technique used in conjunction with isotopic labeling can be employed to probe subtle effects such as the kinetic isotope effects and the stereoselectivity of reactions occurring at the neutral stage. Despite its limitations, we believe that this method opens a new field in mass spectrometric research to the experimentalists as well as theoreticians. The prospect of applying the NIDD method to study the reactivity of radicals which can only be generated by neutralization–reionization mass spectrometry is particularly appealing.

Acknowledgments: We thank Dr. J. N. Harvey for assistance in the preparation of the manuscript. Financial support by the Deutsche Forschungsgemeinschaft, the Fonds der Chemischen Industrie, and the Gesellschaft von Freunden der Technischen Universität Berlin is gratefully acknowledged.

Received: May 2, 1997 [F685]

[1] For the original publication and reviews, see: a) D. H. R. Barton, J. M. Beaton, L. E. Geller, M. M. Pechet, *J. Am. Chem. Soc.* **1961**, *83*, 4076; b) D. H. R. Barton, *Pure Appl. Chem.* **1968**, *16*, 1; c) R. H. Hesse, *Adv. Free-Radical Chem.* **1969**, *3*, 83; d) D. H. R. Barton, R. H. Hesse, M. M. Pechet, L. Smith, *J. Chem. Soc. Perkin Trans.* **1979**, *1*, 1159; e) A. L. J. Beckwith, K. U. Ingold, *Rearrangements in Ground and Excited States* (Ed.: P. DeMayo), Vol. 1, Academic Press, New York, **1980**, p. 251; f) W. Carruthers, *Some Modern Methods of Organic Synthesis*, 3rd ed., Cambridge University Press, Cambridge, **1992**, p. 263.

[2] For a general introduction to the chemistry of free radicals, see: K. U. Ingold, *Pure Appl. Chem.* **1997**, *69*, 241.

[3] a) W. A. Pryor, *Free Radicals*, McGraw Hill, New York, **1966**; b) J. K. Kochi, *Free Radicals* (Ed.: J. K. Kochi), Vol. 2, Wiley, New York, **1973**; c) J. August, M. Brouard, M. P. Docker, C. J. Milne, J. P. Simons, R. Lavi, S. Rosenwaks, D. Schwartz-Lavi, *J. Phys. Chem.* **1988**, *92*, 5485; d) B. Giese, *Methoden Org. Chem. (Houben-Weyl), Vol. E19*, Thieme, Stuttgart, **1989**.

[4] For reviews and recent research, see: a) L. Batt, *Int. Rev. Phys. Chem.* **1987**, *6*, 53; b) R. Atkinson, W. P. L. Carter, *J. Atmos. Chem.* **1991**, *13*, 195; c) R. Atkinson, *J. Phys. Chem. Ref. Data* **1994**, Monograph **2**, 1; d) R. Atkinson, E. S. C. Kwok, J. Arey, S. M. Aschmann, *Faraday Discuss. Chem. Soc.* **1995**, *100*, 23; e) R. Atkinson, S. M. Aschmann, *Environ. Sci. Technol.* **1995**, *29*, 528; f) E. S. C. Kwok, J. Arey, R. Atkinson, *J. Phys. Chem.* **1996**, *100*, 214; g) E. S. C. Kwok, R. Atkinson, J. Arey, *Environ. Sci. Technol.* **1996**, *30*, 1048.

[5] M. M. Green, B. A. Boyle, M. Vairamani, T. Mukhopadhyay, W. H. Saunders, Jr., P. Bowen, N. L. Allinger, *J. Am. Chem. Soc.* **1986**, *108*, 2381.

[6] a) K. Levsen, *Fundamental Aspects of Organic Mass Spectrometry*, VCH, Weinheim, **1978**; b) *Tandem Mass Spectrometry* (Ed.: F. W. McLafferty), Wiley, New York, **1983**; c) *Techniques for the Study of Ion–Molecule Reactions* (Eds.: J. W. Farrar, W. H. Saunders), Wiley, New York, **1988**.

[7] a) R. Lavertu, M. Catte, A. Penenero, P. LeGoff, *C. R. Acad. Sci. Ser. C* **1966**, *236*, 1099; b) F. M. Devienne, *Entropie* **1968**, *24*, 35.

[8] For reviews dealing with NR techniques, see: a) G. I. Gellene, R. F. Porter, *Acc. Chem. Res.* **1983**, *16*, 200; b) C. Wesdemiotis, F. W. McLafferty, *Chem. Rev.* **1987**, *87*, 485; c) J. K. Terlouw, H. Schwarz, *Angew. Chem.* **1987**, *99*, 829; *Angew. Chem. Int. Ed. Engl.* **1987**, *26*, 805; d) J. L. Holmes, *Mass Spectrom. Rev.* **1989**, *8*, 513; e) J. L. Holmes, *Adv. Mass Spectrom.* **1989**, *11*, 53; f) J. K. Terlouw, *ibid.* **1989**, *11*, 984; g) A. W. McMahon, S. K. Chowdhury, A. G. Harrison, *Org. Mass Spectrom.* **1989**, *24*, 620; h) H. Schwarz, *Pure Appl. Chem.* **1989**, *61*, 685; i) F. W. McLafferty, *Science* **1990**, *247*, 925; j) F. W. McLafferty, *Int. J. Mass Spectrom. Ion Processes* **1992**, *118/119*, 221; k) F. Turecek, *Org. Mass Spectrom.* **1992**, *27*, 1087; l) N. Goldberg, H. Schwarz, *Acc. Chem. Res.* **1994**, *27*, 347; m) D. V. Zagorevskii, J. L. Holmes, *Mass Spectrom. Rev.* **1994**, *13*, 133; n) M. J. Polce, Š. Beranová, M. J. Nold, C. Wesdemiotis, *J. Mass Spectrom.* **1996**, *31*, 1073; o) C. A. Schalley, G. Hornung, D. Schröder, H. Schwarz, *Chem. Soc. Rev.*, submitted for publication.

[9] a) P. Fournier, J. Appell, F. C. Fehsenfeld, J. Durup, *J. Phys. B* **1972**, *5*, L58; b) F. C. Fehsenfeld, J. Appell, P. Fournier, J. Durup, *J. Phys. B* **1973**, *6*, L268; c) J. C. Lorquet, B. Leyh-Nihaut, F. W. McLafferty, *Int. J. Mass Spectrom. Ion Processes* **1990**, *100*, 465.

[10] a) C. E. C. A. Hop, J. L. Holmes, *Int. J. Mass Spectrom. Ion Processes* **1991**, *104*, 213; b) D. W. Kuhns, F. Turecek, *Org. Mass Spectrom.* **1994**, *29*, 463; c) D. W. Kuhns, T. B. Tran, S. A. Shaffer, F. Turecek, *J. Phys. Chem.* **1994**, *98*, 4845; d) S. A. Shaffer, F. Turecek, *J. Am. Chem. Soc.* **1994**, *116*, 8647; e) F. Turecek, M. Gu, C. E. C. A. Hop, *J. Phys. Chem.* **1995**, *99*, 2278; f) M. Sadílek, F. Turecek, *ibid.* **1996**, *100*, 224; g) *ibid.*, 9610; h) *ibid.*, 15027; i) M. Sadílek, F. Turecek, *Chem. Phys. Lett.* **1996**, *263*, 203; j) S. A. Shaffer, M. Sadílek, F. Turecek, C. E. C. A. Hop, *Int. J. Mass Spectrom. Ion Processes* **1996**, *160*, 137; k) V. Q. Nguyen, F. Turecek, *J. Mass Spectrom.* **1996**, *31*, 1173;

  0947-6539/97/0311-1881 $ 17.50+.50/0

l) V. Q. Nguyen, F. Turecek, *ibid.* **1997**, *32*, 55; m) V. Q. Nguyen, F. Turecek, *J. Am. Chem. Soc.* **1997**, *119*, 2280; n) D. Schröder, N. Goldberg, W. Zummack, H. Schwarz, J. C. Poutsma, R. R. Squires, *Int. J. Mass Spectrom. Ion Processes*, in press.

[11] For a review, see: M. M. Bursey, *Mass Spectrom. Rev.* **1990**, *9*, 555.

[12] Differences between NR and CR mass spectra have earlier been attributed to neutral reactivity. See, for example: a) P. E. O'Bannon, D. Sülzle, W. P. Dailey, H. Schwarz, *J. Am. Chem. Soc.* **1992**, *114*, 344; b) D. Schröder, C. A. Schalley, N. Goldberg, J. Hrušák, H. Schwarz, *Chem. Eur. J.* **1996**, *2*, 1235; c) C. A. Schalley, A. Fiedler, G. Hornung, R. Wesendrup, D. Schröder, H. Schwarz, *ibid.* **1997**, *3*, 626; d) C. A. Schalley, *Ph.D. Thesis*, Technische Universität Berlin, D83, **1997**.

[13] A detailed description of the method will appear soon in which several methodological problems only briefly mentioned here will be discussed explicitly: C. A. Schalley, G. Hornung, D. Schröder, H. Schwarz, *Int. J. Mass Spectrom. Ion Processes*, in press.

[14] a) R. A. More O'Ferrall, *J. Chem. Soc. B* **1970**, 785; b) A. E. Dorigo, K. N. Houk, *J. Am. Chem. Soc.* **1987**, *109*, 2195; c) A. E. Dorigo, K. N. Houk, *J. Org. Chem.* **1988**, *53*, 1650; d) A. E. Dorigo, M. A. McCarrick, R. J. Loncharich, K. N. Houk, *J. Am. Chem. Soc.* **1990**, *112*, 7508.

[15] P. Gray, R. Shaw, J. C. J. Thynne, *Prog. React. Kinet.* **1967**, *4*, 65.

[16] a) R. Srinivas, D. Sülzle, T. Weiske, H. Schwarz, *Int. J. Mass Spectrom. Ion Processes* **1991**, *107*, 368; b) R. Srinivas, D. Sülzle, W. Koch, C. H. DePuy, H. Schwarz, *J. Am. Chem. Soc.* **1991**, *113*, 5970; c) C. A. Schalley, D. Schröder, H. Schwarz, *Int. J. Mass Spectrom. Ion Processes* **1996**, *153*, 173.

[17] As suggested in ref. [8 d], the charges of projectile and recovery ions are indicated by superscripts.

[18] a) S. W. Froelicher, B. S. Freiser, R. R. Squires, *J. Am. Chem. Soc.* **1986**, *108*, 2853; b) S. T. Graul, R. R. Squires, *ibid.* **1988**, *110*, 607.

[19] K. L. Busch, G. L. Glish, S. A. McLuckey, *Mass Spectrometry/Mass Spectrometry: Techniques and Applications of Tandem Mass Spectrometry*, VCH, Weinheim, **1988**.

[20] J. L. Holmes, *Org. Mass Spectrom.* **1985**, *20*, 169.

[21] GAUSSIAN94, Revision B3: M. J. Frisch, G. W. Trucks, H. B. Schlegel, P. M. W. Gill, B. G. Johnson, M. A. Robb, J. R. Cheeseman, T. Keith, G. A. Peterson, J. A. Montgomery, K. Raghavachari, M. A. Al-Laham, V. G. Zakrzewski, J. V. Ortiz, J. B. Foresman, C. Y. Peng, P. Y. Ayala, W. Chen, M. W. Wong, J. L. Andres, E. S. Replogle, R. Gomperts, R. L. Martin, D. J. Fox, J. S. Binkley, D. J. Defrees, J. Baker, J. P. Stewart, M. Head-Gordon, C. Gonzales, J. A. Pople, GAUSSIAN, Pittsburgh, PA, **1995**.

[22] R. Krishnan, J. S. Binkley, R. Seeger, J. A. Pople, *J. Chem. Phys.* **1980**, *72*, 650.

[23] a) G. Rauhut, R. Pulay, *J. Phys. Chem.* **1995**, *99*, 3093; b) A. P. Scott, L. Radom, *ibid.* **1996**, *100*, 16502.

[24] If not stated otherwise, all thermochemical data have been taken from: a) S. G. Lias, J. E. Bartmess, J. F. Liebman, J. L. Holmes, R. D. Levin, W. G. Mallard, *Gas-Phase Ion and Neutral Thermochemistry, J. Phys. Chem. Ref. Data, Suppl. 1*, **1988**; b) S. G. Lias, J. F. Liebman, R. D. Levin, S. A. Kafafi, *NIST Standard Reference Database, Positive Ion Energetics, Version 2.01*, Gaithersburg, MD, **1994**; c) J. E. Bartmess, *NIST Standard Reference Database, Negative Ion Energetics, Version 3.01*, Gaithersburg, MD, **1993**; d) S. G. Lias, J. F. Liebman, R. D. Levin, *J. Phys. Chem. Ref. Data* **1984**, *13*, 695.

[25] P. M. W. Gill, B. G. Johnson, J. A. Pople, *Chem. Phys. Lett.* **1992**, *197*, 499.

[26] J. M. Galbraith, H. F. Schaefer III, *J. Chem. Phys.* **1996**, *105*, 862.

[27] M. M. Bursey, J. R. Hass, D. J. Harven, C. E. Parker, *J. Am. Chem. Soc.* **1979**, *101*, 5485.

[28] P. C. Burgers, J. L. Holmes, *Org. Mass Spectrom.* **1984**, *19*, 452, and references cited therein.

[29] See, for example: a) K. Hiraoka, P. Kebarle, *J. Am. Chem. Soc.* **1977**, *99*, 366; b) M. J. S. Dewar, H. S. Rzepa, *ibid.* **1977**, *99*, 7432; c) W. J. Bouma, R. H. Nobes, L. Radom, *Org. Mass Spectrom.* **1982**, *17*, 315; d) B. Ruscic, J. Berkowitz, *J. Chem. Phys.* **1991**, *95*, 4033; e) G. Hvistendahl, E. Uggerud, *Org. Mass Spectrom.* **1991**, *26*, 67; f) E. Uggerud, T. Helgaker, *J. Am. Chem. Soc.* **1992**, *114*, 4265.

[30] C. Wesdemiotis, B. Leyh, A. Fura, F. W. McLafferty, *J. Am. Chem. Soc.* **1990**, *112*, 8655.

[31] G. F. Adams, R. J. Bartlett, G. D. Purvis, *Chem. Phys. Letters* **1982**, *87*, 311.

[32] From each decomposition of the intermediate neutrals, one expects two positive signals with correlating intensities in the $^{-}$NIDD^{+} spectrum. For example, α-C–C cleavage of neutral ethoxy radicals is expected to give rise to positive signals for CH_3^+ and $CH_2O^{\cdot+}$. This is, however, not observed for ethoxy radicals due to several effects: a) reionized triplet ethoxy cations contribute to the CH_3^+ signal, in part compensating the positive NIDD intensities; b) different kinetic energies and reionization cross-sections of the fragments affect the reionization efficiencies, which are lower for smaller particles; c) due to thermochemistry, α-C–C cleavage in the cation upon charge inversion preferentially gives rise to CH_3^+ rather than $CH_2O^{\cdot+}$. Finally, isobaric interferences have been observed for some alkoxy radicals, e.g. CH_2OH^+ and $C_2H_3D_2^+$.

[33] R. Breslow, *Acc. Chem. Res.* **1980**, *13*, 170.

[34] a) S. Hammerum, *Mass Spectrom. Rev.* **1988**, *7*, 123; b) K. M. Stirk, L. K. M. Kiminkinen, H. I. Kenttämaa, *Chem. Rev.* **1992**, *92*, 1649; c) H. I. Kenttämaa, *Org. Mass. Spectrom.* **1994**, *29*, 1; d) R. L. Smith, P. K. Chou, H. I. Kenttämaa, *The Structure, Energetics and Dynamics of Organic Ions* (Eds.: T. Baer, C. Y. Ng, I. Powis), Wiley, New York, **1996**.

[35] A. Heiss, K. Sahetchian, *Int. J. Chem. Kinen.* **1996**, *28*, 531.

[36] R. S. Mercer, A. G. Harrison, *Can. J. Chem.* **1988**, *66*, 2947, and references cited therein.

[37] D. P. Stevenson, *Discuss. Faraday Soc.* **1951**, *10*, 35.

[38] It is not known exactly which of the possible C_4H_8 isomers is formed (see discussion of the potential energy surface depicted in Figure 8). However, all C_4H_8 isomers listed in ref. [24] have ionization energies of more than 9 eV.

[39] Several previous studies provided experimental and theoretical evidence for a remarkably high regioselectivity of this process, which is due not only to enthalpic but also to entropic effects. For examples, see refs. [1,5,14].

[40] For a discussion of the role of bent hydrogen bonds in proton transfers, see: S. Scheiner, *Acc. Chem. Res.* **1994**, *27*, 402.

[41] Rearrangement reactions in reionized cations stemming from charge reversal or neutralization reionization experiments are, of course, known and have previously been described. See, for example: N. Goldberg, A. Fiedler, H. Schwarz, *J. Phys. Chem.* **1995**, *99*, 15334, and references therein.

[42] a) D. F. McMillen, D. M. Golden, *Ann. Rev. Phys. Chem.* **1982**, *33*, 493; b) J. March, *Advanced Organic Chemistry*, 4th ed., Wiley, New York, **1992**, p.24.

[43] An activation energy in the range of 8–11 kcal mol^{-1} for the hydrogen transfer in the Barton reaction is discussed in: C. Wentrup, *Reaktive Zwischenstufen I*, Thieme, Stuttgart, **1979**.

[44] J. W. Wilt, *Free Radicals, Vol. 1* (Ed.: J. K. Kochi), Wiley, New York, **1973**, p. 333.

[45] Reaction channels above the threshold defined by the energy demand of the α-cleavage may occur upon collisional activation of the radicals. Thus, the formation of $^{\cdot}CH_2OH$ radicals concomitant with C_4H_8, a rather unusual fragmentation for **9**$^{\cdot}$, may also be due to contributions of collision processes following the 1,5-hydrogen migration.

[46] S. Dua, G. W. Adams, J. C. Sheldon, J. H. Bowie, *J. Chem. Soc. Perkin Trans. 2* **1996**, 1251.

[47] K. N. Houk, Y. Li, J. D. Evanseck, *Angew. Chem. Int. Ed. Engl.* **1992**, *31*, 682.

[48] a) D. J. McAdoo, F. W. McLafferty, P. F. Bente, III, *J. Am. Chem. Soc.* **1972**, *94*, 2027; b) W. Koch, P. v. R. Schleyer, P. Buzek, B. Liu, *Croat. Chim. Acta* **1992**, *65*, 655.

[49] a) T. H. Morton, *Tetrahedron* **1982**, *38*, 3195; b) N. Heinrich, H. Schwarz, *Ion and Cluster Ion Spectroscopy and Structure* (Ed.: J. P. Maier), Elsevier, Amsterdam, **1989**, p. 329, and references therein; c) R. D. Bowen, *Acc. Chem. Res.* **1991**, *24*, 364; d) P. Longevialle, *Mass Spectrom. Rev.* **1992**, *11*, 157; e) D. K. Böhme, *Int. J. Mass Spectrom. Ion Processes* **1992**, *115*, 95.

[50] For applications of mass spectrometry to stereochemical problems in connection with the decay of metastable ions, see: a) Y. S. Nekrasov, D. V. Zagorevskii, *Org. Mass Spectrom.* **1991**, *26*, 733; b) T. Prüsse, A. Fiedler, H. Schwarz, *Helv. Chim. Acta* **1991**, *74*, 1127; c) K. Seemeyer, T. Prüsse, H. Schwarz, *ibid.* **1993**, *76*, 1632; d) K. Seemeyer, T. Prüsse, H. Schwarz, *ibid.* **1993**, *76*, 113; e) K. Seemeyer, H. Schwarz, *ibid.* **1993**, *76*, 2384; f) N. Raabe, S. Karrass, H. Schwarz, *Chem. Ber.* **1994**, *127*, 261; g) C. A. Schalley, D. Schröder, H. Schwarz, *J. Am. Chem. Soc.* **1994**, *116*, 11089; h) *Applications of Mass Spectrometry to Organic Stereochemistry* (Eds:. J. S. Splitter, F. Turecek), VCH, Weinheim, **1994**; i) K. Schroeter, C. A. Schalley, R. Wesendrup, D. Schröder, H. Schwarz, *Organometallics*, **1997**, *16*, 986.

[51] a) D. Schröder, *Ph.D. Thesis*, Technische Universität Berlin, D83, **1992**; b) D. Schröder, H. Schwarz, *J. Am. Chem. Soc.* **1993**, *76*, 8818; c) G. Hornung, D. Schröder; H. Schwarz, *ibid.* **1995**, *117*, 8192; d) G. Hornung, D. Schröder, H. Schwarz, *ibid.* **1997**, *119*, 2273.

[52] The branching ratios are given without statistical corrections for the number of H/D atoms and neglecting the kinetic isotope effect, as their influence on the estimated value for the site selectivity is not significant.

[53] Assuming that the isotope effects associated with H/D transfer are identical, irrespective of the relative configuration of the methyl groups in **TS 8**$^{\cdot}$/**16**$^{\cdot}$, the following equations can be derived. The kinetic isotope effect [KIE, Eq. (2)] disfavors the transfer of a deuterium atom, while the steric effect [SE, Eq. (3)]

$$\mathrm{KIE} = \frac{k_\mathrm{H}}{k_\mathrm{D}} \tag{2}$$

$$\mathrm{SE} = \frac{k_\mathrm{eq}}{k_\mathrm{ax}} \tag{3}$$

is due to the presence of an equatorial or axial methyl group in a chairlike, six-membered transition structure. These definitions lead to the expression in Equation (4) for the ratio of hydrogen versus deuterium transfer for **8e**$^{\cdot}$, where

$$\frac{I_\mathrm{H}}{I_\mathrm{D}} = \frac{k_\mathrm{H} \cdot k_\mathrm{eq}}{k_\mathrm{D} \cdot k_\mathrm{ax}} = \mathrm{KIE} \cdot \mathrm{SE} \tag{4}$$

the C(5) methyl group is equatorial during the H-shift and axial if D is transferred. In analogy, for the diastereoisomer **8f**$^{\cdot}$ Equation (5) is derived; here, the

$$\frac{I'_\mathrm{H}}{I'_\mathrm{D}} = \frac{k_\mathrm{H} \cdot k_\mathrm{ax}}{k_\mathrm{D} \cdot k_\mathrm{eq}} = \frac{\mathrm{KIE}}{\mathrm{SE}} \tag{5}$$

  0947-6539/97/0311-1882 $ 17.50+.50/0

C(5) methyl group is axial upon H transfer and equatorial during the D migration: By combining Equations (4) and (5), the KIE can easily be separated from the SE [Eqs. (6) and (7)] as follows: The ratios of the intensities I_H/I_D and I'_H/I'_D

$$SE = \sqrt{\left(\frac{I_H \cdot I'_D}{I_D \cdot I'_H}\right)} \quad (6)$$

$$KIE = \sqrt{\left(\frac{I_H \cdot I'_H}{I_D \cdot I'_D}\right)} \quad (7)$$

are derived from the intensities of CH_2OH^+ versus CH_2OD^+ ions in the two $^-NIDD^+$ mass spectra depicted in Figures 11 and 12 for **8e**$^\bullet$ and **8f**$^\bullet$, respectively. As average of several independent measurements we obtain Expressions (8) and (9), respectively, for **8e**$^\bullet$ and **8f**$^\bullet$. In combination with Equations (6) and (7) the kinetic isotope and the steric effects can be estimated.

$$\frac{I_H}{I_D} = \frac{87}{13} = 6.69 \quad (8)$$

$$\frac{I'_H}{I'_D} = \frac{33}{67} = 0.49 \quad (9)$$

[54] Taking into account the reaction path proceeding via **TS8**$^\bullet$/**17**$^\bullet$ (Scheme 7), which contributes with $\approx 14\%$ to the formation of CH_2OH^+ from **8e**$^\bullet$ and **8f**$^\bullet$, we obtain the following corrected values for the kinetic isotope and the steric effects: SE $= 3.7 \pm 1.3$ and KIE $= 1.5 \pm 0.3$. Thus, the qualitative picture is not significantly altered by this side reaction.

[55] For the sake of clarity, in Scheme 8 only the reactions of one enantiomer of the racemic pair **8e**$^-$ are shown. For the diastereoisomer **8f**$^-$ all essential features are identical, except that the H/CH_3 substituents in the C(3) position are interchanged.

  0947-6539/97/0311-1883 $ 17.50+.50/0